NASA CR-134629
FR-6353

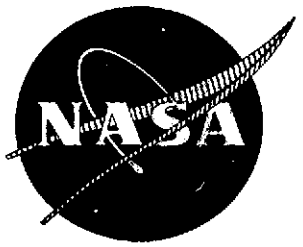

DEVELOPMENT OF SPUTTERED TECHNIQUES FOR THRUST CHAMBERS

TASK I - FINAL REPORT

March 1974

by: J. R. Mullaly, T. E. Schmid, R. J. Hecht

Pratt & Whitney Aircraft
Division of United Aircraft Corporation

National Aeronautics and Space Administration

NASA-Lewis Research Center
Contract NAS3-17792

1. Report No.	2. Government Accession No.	3. Recipient's Catalog No.
NASA CR-134629		

4. Title and Subtitle	5. Report Date
Development of Sputtered Techniques for Thrust Chambers Task I Final Report	March 1974
	6. Performing Organization Code

7. Author(s)	8. Performing Organization Report No.
J. R. Mullaly, T. E. Schmid, and R. J. Hecht	FR-6353
	10. Work Unit No.

9. Performing Organization Name and Address	11. Contract or Grant No.
Pratt & Whitney Aircraft Florida Research and Development Center P. O. Box 2691 West Palm Beach, Florida 33402	NAS3-17792
	13. Type of Report and Period Covered
12. Sponsoring Agency Name and Address	Contractor Report
National Aeronautics and Space Administration Washington, D. C. 20546	14. Sponsoring Agency Code

15. Supplementary Notes

John Kazaroff, Project Manager
NASA Lewis Research Center,
Cleveland, Ohio 44135

16. Abstract

The purpose of this program was to evaluate filler materials proposed for use in the sputter fabrication of regeneratively cooled thrust chambers. Low melting castable alloys, CERROBEND®, CERROCAST®, and CERROTRU®, slurry applied SERMETEL® 481 and flame-sprayed aluminum were investigated as filler materials. Sputter deposition from a cylindrical cathode inverted magnetron was used to apply an OFHC copper closeout layer to filled OFHC copper ribbed-wall cylindrical substrates. The sputtered closeout layer structure was evaluated with respect to filler material contamination, predeposition machining and finishing operations, and deposition parameters.

The application of aluminum by flame-spraying resulted in excessive filler porosity. Though the outgassing from this porosity was found to be detrimental to the closeout layer structure, bond strengths in excess of 73.2 MN/m^2 (10,500 psi) were achieved. Removal of the aluminum from the grooves was readily accomplished by leaching in a 7.0 molar solution of sodium hydroxide at 353°K.

Of the other filler materials evaluated, CERROTRU was found to be the most suitable material with respect to completely filling the ribbed-wall cylinders and vacuum system compatibility. However, bond contamination resulted in low closeout layer bond strength with the CERROTRU filler. Bond strengths ranging from 0.69 MN/m^2 (100 psi) to 67.6 MN/m^2 (9800 psi) were attained.

CERROBEND, CERROCAST, and SERMETEL 481 were found to be unacceptable as filler materials.

17. Key Words (Suggested by Author(s))	18. Distribution Statement
Sputtering Thrust Chambers OFHC Copper Flame spraying CERROTRU®	Unclassified - Unlimited

19. Security Classif. (of this report)	20. Security Classif. (of this page)	21. No. of Pages	22. Price*
Unclassified	Unclassified	54	$6.50

* For sale by the National Technical Information Service, Springfield, Virginia 22151

TABLE OF CONTENTS

LIST OF ILLUSTRATIONS

LIST OF ILLUSTRATIONS (Continued)

LIST OF TABLES

INTRODUCTION

In the development of advanced chambers for programs such as the Space Tug Experimental Engine Program, new fabrication techniques and/or materials will be needed to meet the projected chamber requirements. Of the techniques currently available for fabrication, deposition by sputtering offers the most potential of meeting the demands of the advanced designs. The application of sputtering techniques to the fabrication of thrust chambers permits relative freedom in materials selection for the chamber designer. Not being limited by the inability to electrodeposit a material and not having to sacrifice the material properties by elevated temperature joining operations, the chamber can be fabricated from practically any alloy or combination of alloys desired. Furthermore, the improved bonding obtainable with sputtering provides increased low-cycle fatigue life through improved materials and an elimination of joining materials at the bond interface. Previous work by McClanahan, Busch and Moss[1] has shown that precipitation-hardened and dispersion-strengthened copper alloys synthesized by sputtering offer potential as materials for fabricating regeneratively cooled thrust chambers. Furthermore, it was shown that a sputtered copper-0.15 zirconium alloy can be stronger than the same alloy produced by conventional primary forming techniques.

The proposed method for chamber fabrication by sputtering involves the sputtering of an inner wall or inner chamber jacket, which is machined to a ribbed wall configuration. The chamber channels are then filled with a suitable material and the final closeout layer applied. Fabrication by this approach requires that the filler material be compatible with the vacuum sputtering environment. The filler must be capable of being applied to the channeled configuration and completely removed without degrading the chamber material properties. The inner wall structure and closeout layer could be (1) an alloy such as copper-0.15 zirconium; (2) a dispersion-strengthened, high-strength copper alloy; or (3) made of graded layers to promote improved fatigue capabilities. The sputter application of a high strength alloy outer chamber structure, with or without wire reinforcement, may permit further increases in chamber pressure to be attained, as indicated by the work of McCandless and Davies.[2] Sputtering of inner wall coatings for refurbishment or surface protection are further concepts for extending chamber life. It is the objective of this program to develop sputtering techniques for evaluating these concepts of advanced chamber fabrication.

The investigation to be performed in this program is divided into five work tasks. Task I involves the application of an OFHC copper closeout layer to a ribbed wall cylinder to yield a cylindrical structure representative of regeneratively cooled thrust chambers. Within this task an investigation of materials to fill the grooved cylinder passages and selection of predeposition processing and sputtering deposition parameters compatible with the filler materials will be performed. With the techniques developed, a cylindrical channeled structure will be fabricated and evaluated for closeout layer bond strength and bond integrity. In Task II, fabrication and evaluation of 0.625 cm (0.250 in.) thick wall cylinders of sputtered OFHC Cu, Zr-Cu, Al_2O_3-Cu, and SiC-Cu will be performed. With the cylinders fabricated, an investigation of structure, hardness, and tensile properties of each alloy will be determined. The purpose of Task III is to investigate sputtering laminated cylindrical structures. One cylinder will

be sputtered with four layers of the same material, the other with each layer of a different composition or a different hardness of the same composition. The materials for this task will be selected by NASA-LeRC from those evaluated in the second task of this program. Each cylinder will be evaluated for layer hardness, structure, bond integrity, and bond strength. Higher strength outer structures will be evaluated in Task IV. Three sputtered alloys, NASA IIb-11, Ti-5Al-2.5Sn, and an aluminum alloy will be evaluated for tensile properties. Upon NASA-LeRC selection of one of these alloys, a homogeneous cylindrical structure will be fabricated from the selected alloy and evaluated for tensile and burst strength. A second sputtered cylinder having wire reinforcement of the matrix alloy selected will be burst tested to determine if the strength advantage of wire reinforcement can be achieved on sputtered structures. Task V of the program will investigate techniques for refurbishment and coating of the inner surface of thrust chambers.

Inner surfaces of 7.6 cm (2.6 in.) internal diameter OFHC cylinders will be sputtered with OFHC copper, ZrO_2 and graded OFHC copper - ZrO_2 coatings. These will be evaluated for hardness, bond quality, and bond integrity.

This report covers the evaluation performed in Task I of this program. The remaining program developments and evaluations will be presented in the program final report.

EQUIPMENT AND PROCEDURES

The equipment used for sputter deposition is shown schematically in figure 1. The vacuum chamber was of welded stainless steel construction, with elastomer sealed main flanges. All other flanges were metal sealed. The vacuum pumping system consisted of an air-driven aspirator pump, two liquid-nitrogen-cooled sorption pumps, and a 0.270 m^3/s ion pump. The target, substrate, and anode (for triode operation) power supplies were all unfiltered fullwave-rectified supplies with a nominal 4.2% ripple. The magnetic coil current was provided by a filtered dc supply with a nominal 1% ripple. The filament current was provided by an ac power supply.

The targets, machined from Certified Grade 101 OFHC copper, [3] were 14.6 cm long with an outside diameter of 12.7 cm. Target internal diameters of 10.2, 11.4 and 11.7 cm were employed in the depositions performed. The targets were supported in a water-cooled stainless steel holder. Cylindrical substrates were held on a stainless steel or OFHC copper holder, water-cooled through a coaxial support tube.

Two chromel-alumel thermocouples were attached to the cylinder to monitor temperature during deposition. The end of one thermocouple was bolted between the substrate holder cap and the end of the substrate cylinder, while the other was tied to the cylinder surface 0.6 cm below the other thermocouple and 180 degrees from it. No attempt was made to relate this thermocouple reading to the actual temperatures of the substrates. The thermocouple attached to the holder cap was used to indicate bulk substrate temperature. The other thermocouple, exposed to the discharge and not in true intimate contact with the substrate, was used to indicate if melting of the filler was imminent.

Except for a few of the initial depositions, which used argon, research grade 99.99% pure krypton[4] was employed as the sputtering gas. Pressure during sputtering was measured with a Pirani gauge, and the gauge reading corrected to the approximate krypton pressure. A Schultz-Phelps gauge was employed to detect rapid changes in pressure and served as a backup gauge. The ion pump current was used to indicate pumpdown pressure.

The operational characteristics of the sputtering device did not depend greatly on substrate diameter. The selected substrate diameter of 6.1 cm was within the 5.1 to 7.6 cm requirement and minimized the machining required on the starting substrate material.

The substrates for evaluation were machined from Certified Grade 101 OFHC copper[3] tubing. Two configurations of cylindrical substrates were fabricated: fully grooved (figure 2) and quarter-grooved (figure 3). The blank cylinder was mounted on an aluminum arbor, affixed to an indexing head and the grooves machined using an 0.159-cm wide cutter. The cylinder was approximately 2.5 cm longer and 0.025 cm larger in diameter than the final dimensions desired. The excess length and diameter were machined off after filling to provide a clean surface on the ribs. The final machining and finishing operations were an integral part of the filler material evaluation and will be separately discussed in the following sections.

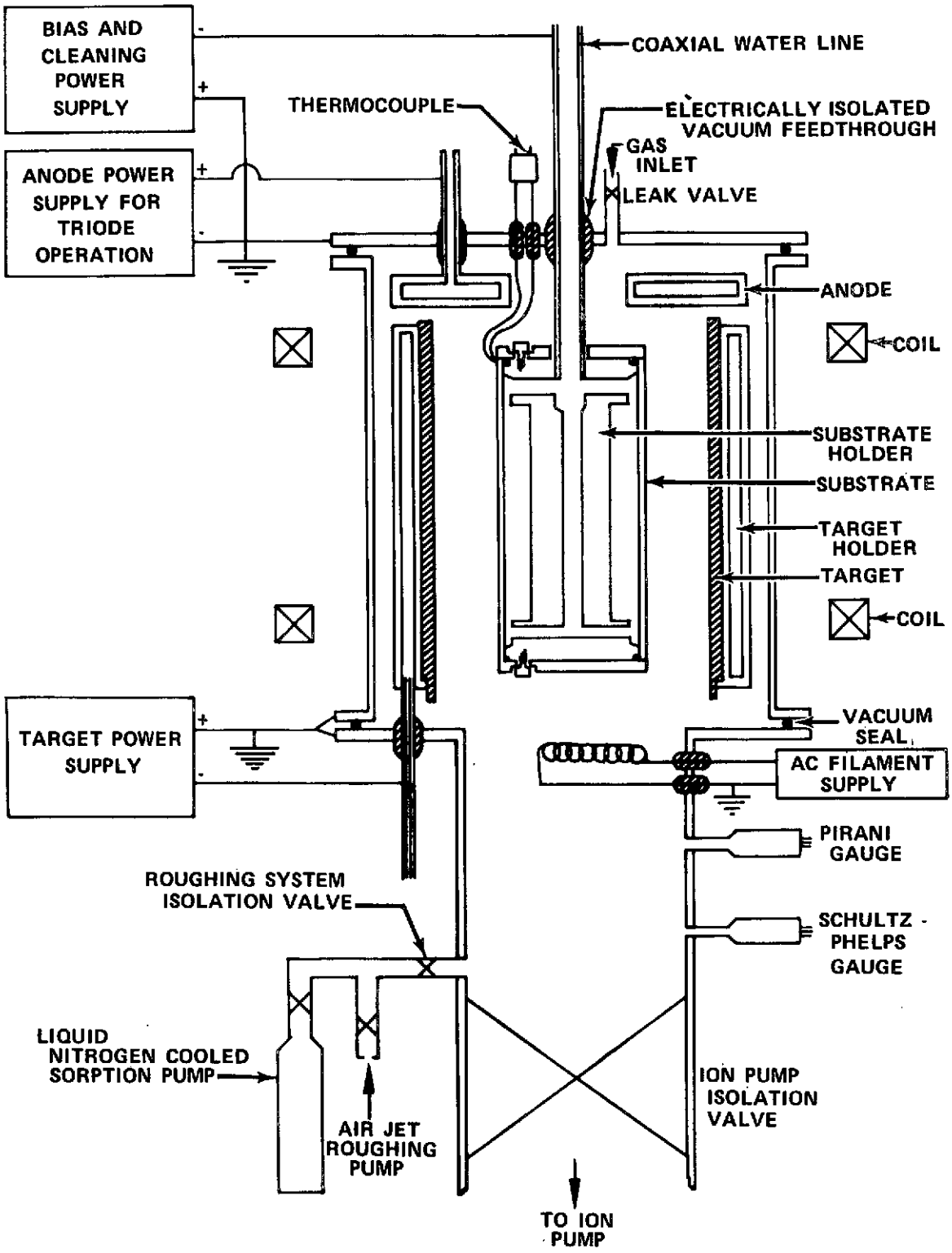

Figure 1. Inverted Magnetron Coater Schematic FD 78478

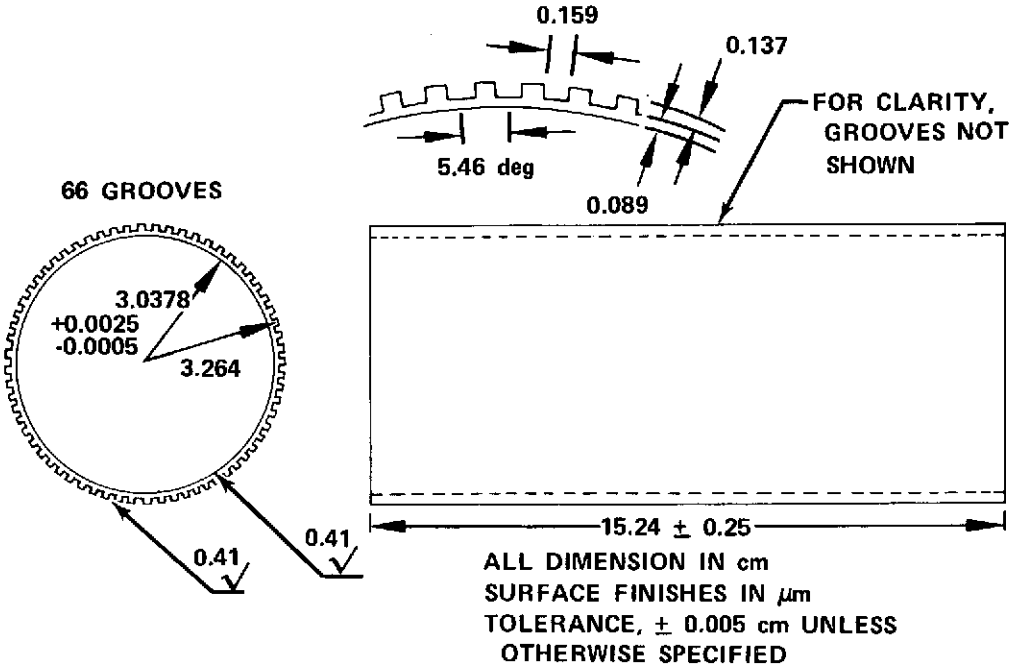

Figure 2. Fully Grooved OFHC Copper Substrate FD 78464

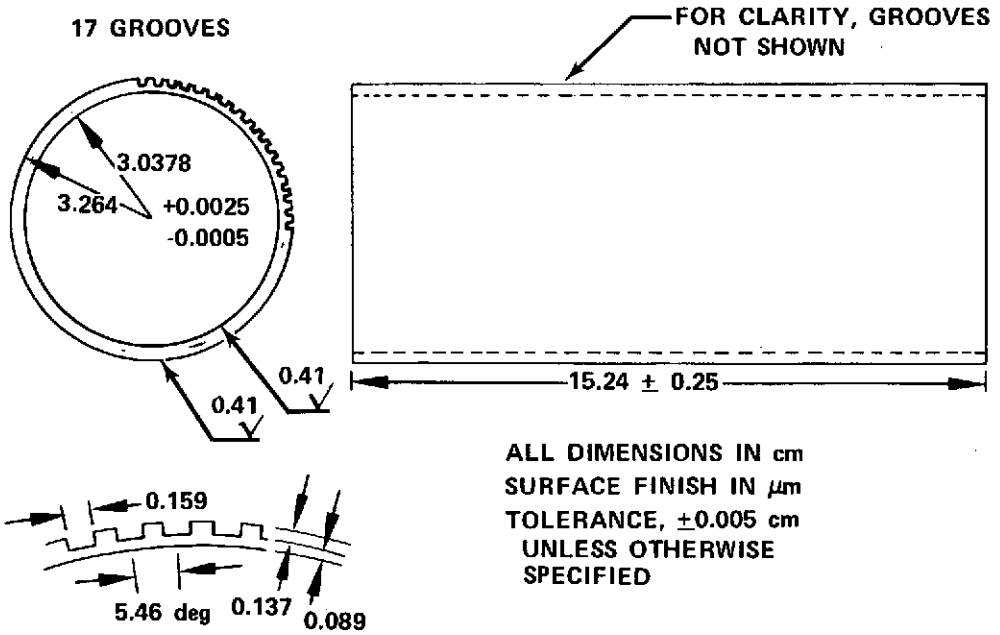

Figure 3. Quarter-Grooved OFHC Copper Substrate FD 78465

A general procedure was used in all depositions performed in this evaluation. The substrate with the desired surface finish was cleaned, installed on the substrate holder, and loaded into the vacuum chamber. The system was then rough pumped with an air-driven aspirator pump and ion pumped to high vacuum. The time required to reach a low base pressure was dependent on the filler material being evaluated.

After pumping to high vacuum, argon or krypton was bled into the system and sputter cleaning (back sputtering) of the substrate started. Argon was used during the initial experiments (runs I-1 through I-9) because the krypton was not available. Krypton was used in the latter runs because of the higher deposition rates resulting when this gas was used. During sputter cleaning, the magnetic field was established and a high negative substrate bias voltage applied. The purpose of the sputter cleaning was to remove gases and other contaminants from the substrate surface so that a high strength substrate-closeout layer bond would be achieved. Substrate cleaning was usually accomplished by several cycles of ion bombardment, followed by pumping to high vacuum. Sputter cleaning the substrate also accomplished a partial cleanup of the target. During the final cleaning cycle, the target was run simultaneously with the substrate. The cleaning cycles were continued until no increase in pressure was noted when the discharge was initiated.

To start deposition, the voltage and current to the target were increased to the desired level. Usually, target power was kept low at the start of deposition to minimize substrate heating and outgassing or vaporizing of the filler material.

From the completed cylinder of each deposition, sections were removed for metallographic examination. These were typically mounted in clear epoxy and polished to a 1μ finish. Etching was performed exclusively with a solution of 5g $FeCl_3$, 10-ml HCl, 50-ml glycerin, and 30-ml water.

When closeout layer bond strength was to be determined, 2.5 by 2.5 cm square sections were removed for tensile testing. After removal of the filler material, these sections were bonded to tensile fixtures (figure 4) with EA951 Structural Adhesive[5] (450°K, 4.5-ks air cure) and pulled in tension normal to the bond interface at a strain rate of 8.3×10^{-5} cm/cm/s (0.005 in./in./min). Where high bond strengths were anticipated, the ribs on each side of the segment were cut to reduce bond area.

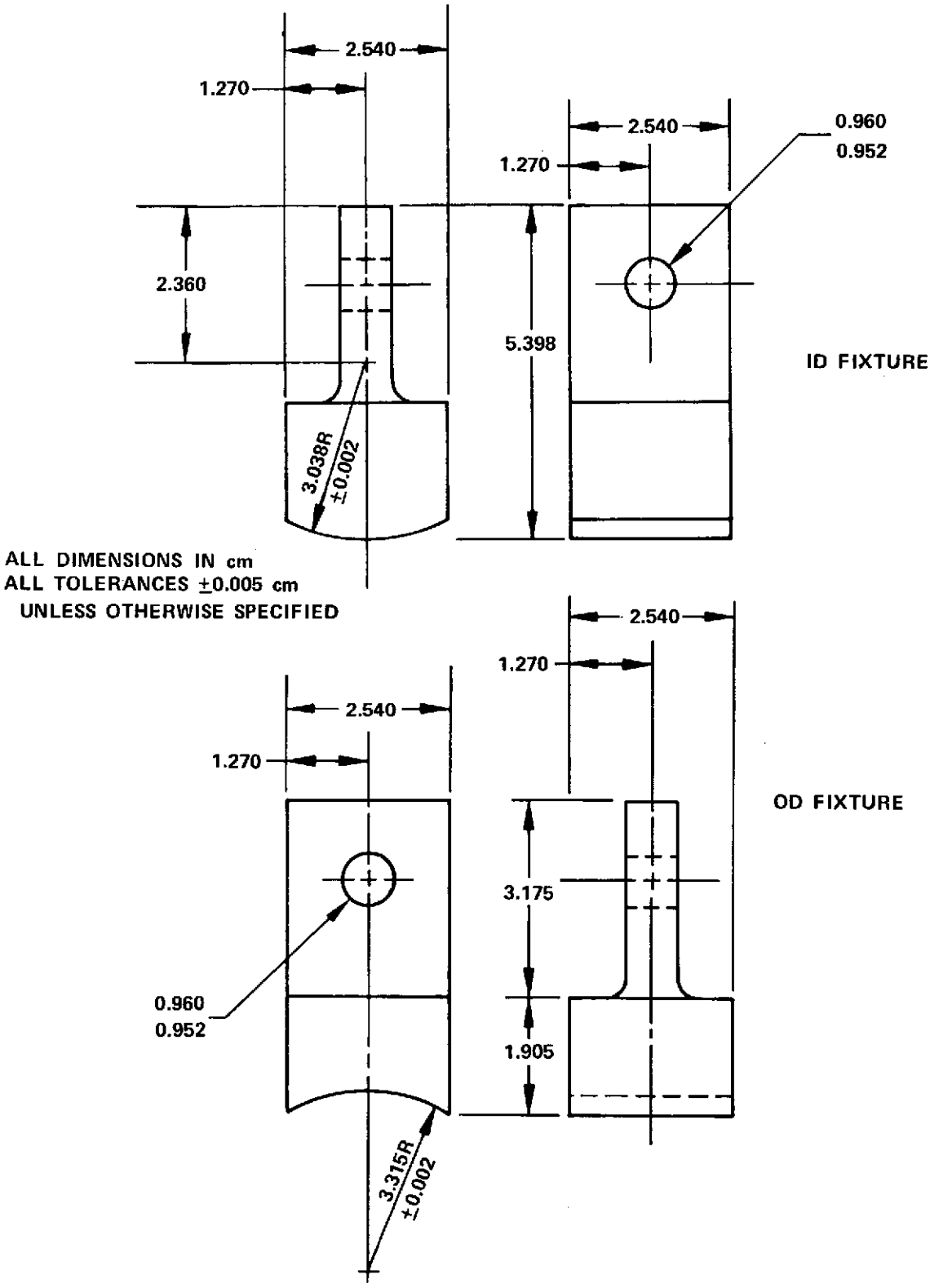

Figure 4. Tensile Fixtures for Determination of Closeout Layer Bond Strength

FD 80757
740107

FILLER MATERIALS

Selection

The filler materials chosen for this evaluation (table I) included materials that could be applied by casting, flame or plasma spraying, or slurry techniques. Casting was to be limited to materials whose melting point was less than 450°K (177°C). Three low melting alloys CERROTRU®, CERROCAST®, and CERROBEND® [6] were selected for evaluation. CERROBEND was chosen for its low melting point and ease of application, while CERROCAST was selected because of its stability after casting and its noneutectic composition providing a nonunique freezing temperature. CERROTRU was selected because its net expansion upon freezing would provide a tighter mechanical bond to the groove walls.

Table I. Filler Materials

Material	Melting Temperature, °K	°F	Composition, Percent by Weight
CERROBEND®	343	158	50Bi-26.7Pb-13.3Sn-10Cd
CERROCAST®	411-443	281-338	40Bi-60Sn
CERROTRU®	411	281	58Bi-42Sn
Aluminum	933	1220	99.9Al
SERMETEL® 481	933	1220	45Al-54.5$NaSiO_4$-0.5ZnO

The SERMETEL® 481 material [7] was selected because of the ease of application. This material is applied as a slurry and dried at 353°K (80°C). Usually, this material is then baked at 811°K (538°C) to sinter the particles together to form a continuous aluminum matrix. This was not to be performed, since this exposure would result in annealing the OFHC copper substrate.

Pure aluminum, applied by flame spraying, provided the final filler material examined. Ranging in density from 85 to 90% of theoretical density, this material could be easily machined and easily removed by leaching in a NaOH solution. Aluminum and SERMETEL 481 allowed higher substrate temperatures to be maintained during deposition of the closeout layer.

Filling Techniques

All CERRO® Alloys examined in this program as possible filler materials were cast into the grooves using the same technique. (See figure 5.) The technique consisted of three steps: preparation of the cylinder, casting of the CERRO Alloy, and removal of the cylinder from the casting.

FOLDOUT FRAME

1

FOLDOUT FRAME

1

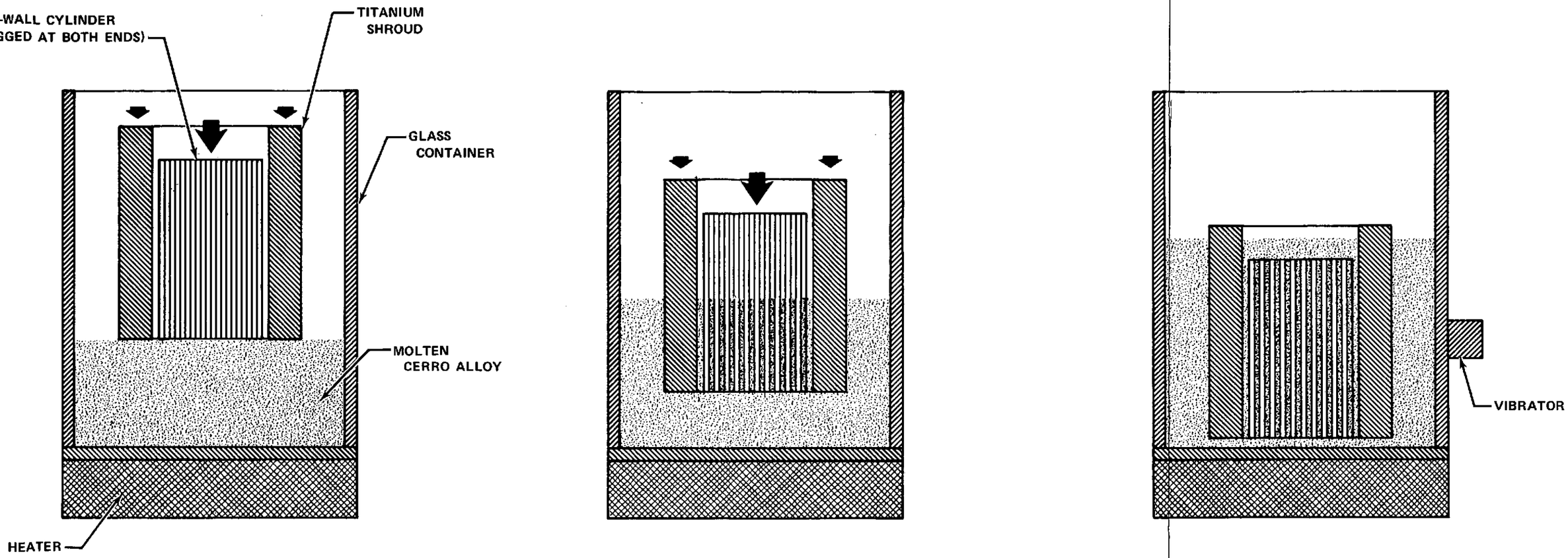

A. PREHEATED CYLINDER AND SHROUD PUSHED VERTICALLY INTO MOLTEN CERRO ALLOY

B. CERRO ALLOY IS FORCED UP THE GROOVE DURING SLOW RATE IMMERSION INTO THE MOLTEN POOL

C. UPON COMPLETE IMMERSION AND FILLING THE GROOVES, THE CYLINDER IS VIBRATED TO REMOVE ENTRAPPED BUBBLES. THE CERRO ALLOY IS THEN ALLOWED TO SOLIDIFY. THE OUTER GLASS CONTAINER, EXCESS CERRO ALLOY, AND TITANIUM SHROUD ARE REMOVED AND THE FILLED CYLINDER MACHINED TO FINAL DIMENSIONS.

Figure 5. Procedure for Filling Ribbed Wall Cylinder With CERRO® Alloys

FD 78171

Typically, the cylinder was prepared by vapor blasting or sanding the grooves to remove burrs and contaminants and washed with methanol. The ends of the cylinder were tightly plugged. The cylinder was then tightly wrapped with 0.0127-cm Ti-6Al-4V sheet so that it extended slightly beyond the copper cylinder ends. The titanium alloy sheet was secured with 0.025-cm diameter wire at two positions along the cylinder length. This assembly was then preheated for 2 to 3 min in an air furnace at 477 ± 10°K (204 ±10°C).

Approximately 3.9 kg of CERRO Alloy was melted in a PYREX® container and the molten alloy skimmed to remove floating contaminants. The preheated cylinder was pushed vertically into the molten CERRO Alloy so that the top edge of the copper cylinder was below the surface of the molten CERRO Alloy. Since a difference in pressure exists, the molten CERRO Alloy is forced up the passages formed by the titanium alloy sheet and the grooved copper cylinder. Vibrating the assembly assisted the movement of entrapped bubbles up the grooves and assured complete filling of the passages. The whole assembly was then allowed to cool to room temperature.

After removing the outer glass container, the excess CERRO Alloy was broken away, and the titanium-alloy sheet and the end plugs removed to complete the process. The filled grooves were visually examined for entrapped porosity and subsequently machined to final dimensions. This entailed removal of 2.54 cm from the cylinder length and 0.0254 cm from the outside diameter.

The aluminum filler material was applied to the vapor-blasted cylinder by flame spraying. After approximately 0.025 cm of aluminum was applied, the excess was removed from the ridges between the grooves. This procedure was continued until the flame-sprayed aluminum completely filled the grooves. The cylinder was then machined to final dimensions. The SERMETEL 481 filler was trowelled into the grooves and baked at 353°K (80°C) for approximately 1 hr. The filled cylinder was then machined to final dimensions.

Machining Operations

The removal of the final 0.025 cm from the diameter of the cylinders after filling was performed using a variety of machining techniques. These included: the normal lathe turning operation, longitudinal surface grinding, longitudinal milling, and bidirectional dry machining. The several techniques were tried in an attempt to minimize smearing of the filler material onto the rib lands and to eliminate the formation of cracks along the grooves due to the filler material being pulled away from one side of the groove. Each operation is described in detail in the following paragraphs.

Normal Lathe Machining - The filled cylinder was mounted on an aluminum arbor, rotated axially at 3 rev/s. Using a carbide cutting tool, traversing at 0.005 cm per revolution, approximately 0.013 cm was removed from the radial dimension per pass during the initial rough machining and approximately 0.002 cm was removed from the radial dimension per pass during the final finishing operation. No lubricants were used at any time during this machining operation. Trimming to length was performed as the final operation in this and all subsequent machining techniques to be discussed.

Longitudinal Surface Grinding - The filled cylinder was mounted on an aluminum arbor attached to an indexing fixture. The surface grinding operation was performed using an AF-1226 grinding wheel, rotating at about 40 rev/s and traversing the specimen lengthwise at 0.1 cm/s. Removal of 0.0013 cm per pass resulted in a flat surface approximately 0.3 cm wide. After each pass the cylinder was rotated 5.46 deg. A water soluble lubricant was used throughout the surface grinding operation.

Longitudinal Milling - The basic setup for the longitudinal milling operation was the same as that used for the surface grinding operation. In this operation, a 1.9-cm diameter carbide end mill rotating at 5 rev/s traversed the cylinder at 0.1 cm/s. The axis of rotation of the end mill was parallel to the tangent plane of the surface being milled and orthogonal to the cylinder axis. The cylinder was rotated 5.46 deg after each pass. After milling, the cylinder had 66 flats approximately 0.3 cm wide about the circumference. A water-soluble lubricant was used in this machining operation.

Bidirectional Dry Machining - The dry machining operation was performed on a reversing lathe with the cylinder mounted on an aluminum arbor and rotated at 2.3 rev/s. Using a TGB 431 cutting tool, traversed at 4.5×10^{-3} cm per revolution, approximately 0.0025 cm was removed per pass. The lathe rotation was reversed for the final two passes. The cylinder was then polished with 600-grit SiC paper in both directions on the lathe to complete the process. No lubricants were used at any time during the dry machining operation.

Finishing Operations

Several techniques were employed throughout this program to eliminate the smearing of the filler material onto the rib lands, reduce the surface porosity of the filler materials, eliminate the pulling of the filler away from one side of the grooves, or affect the surface finish of the substrate. These operations included shot peening, vapor blasting, glass bead peening, chemical polishing, and mechanical polishing, and, in some cases, a sequence of several of these.

Shot Peening - The shot peening was performed using SAE 170 cast steel shot at a carrier air pressure of 0.210 MN/m^2 (30 psi). The orifice was held 3 to 7 cm from the surface. The flow was directed normal to the surface and traversed in such a way that a given point experienced 3 to 5 sec of peening.

Vapor Blasting - The vapor blasting operation was performed using a water slurry of 325-grit NOVACULITE® with a water pressure of 0.55 to 0.69 MN/m^2 (80 to 100 psi). Typically, the nozzle was held approximately 20 cm from and 45 deg inclined to the surface of the cylinder. Vapor blasting was performed until the desired surface finish was achieved.

Glass Bead Peening - The glass bead peening operation was performed using 0.0177- to 0.0296-cm diameter glass beads impinging normal to the surface from a nozzle held 5 to 10 cm from the surface. Typically, the peening operation was performed with a water carrier operating at a line pressure of 0.55 to 0.69 MN/m^2 (80 to 100 psi). The nozzle was traversed at such a rate that a given point on the surface experienced approximately 5 sec of peening.

Chemical Polishing - Chemical polishing was accomplished by placing the work piece in a solution consisting of equal portions of H_3PO_4, CH_3COOH, and HNO_3 for 5 sec. The solution was typically heated to 348 ±5°K. Immersion in distilled water followed by an ethanol rinse completed the process.

Mechanical Polishing - Mechanical polishing was performed using a hand-held, air-operated tool. The polishing media, 6μ paste, was applied to the MICROCLOTH® disk affixed to the polishing tool. A VARSOL® carrier was liberally applied to the work piece throughout the polishing operation. Polishing pressure and direction were left to the discretion of the operator performing the polishing.

The surfaces of many cylinders were finished by sanding with 600-grit SiC paper using no lubricants. Both lengthwise and circumferential sanding were employed, although both were not necessarily used on every cylinder. The sanding operation was continued until the desired surface finish was achieved.

Sputter Cleaning

After the filled cylinder had been machined to final dimensions and the surface finished to the desired degree, a final cleaning was performed prior to insertion in the vacuum chamber. Sputter cleaning (back sputtering) was employed to remove surface contaminants that could degrade the interface between the substrate and the closeout layer. (See table II.) The deposition cycle (table III) immediately followed the sputter cleaning operation. In some cases, the two processes were performed simultaneously, i.e., while one was being phased in the other was being phased out. Whenever the deposition was stopped for any significant period of time, a sputter cleaning cycle was performed prior to re-initiating the deposition cycle.

Filler Removal

Techniques were established for removal of the CERROTRU and aluminum fillers. Removal of the flame-sprayed aluminum by leaching with NaOH was found to be most rapid between 6.0 and 7.0 molarity. (See figure 6.) Ultrasonic vibration and tilting of the sample did not result in significant increases in the rate of removal. A maximum rate of 1.3×10^{-4} m/s (0.48 cm/hr) was obtained using 7.0 molar NaOH at 348 to 353°K (75 to 80°C) without ultrasonic vibration. Removal of the CERROTRU was accomplished by placing one end of the cylinder in a pool of molten CERROTRU at 453°K (180°C) for about 300 seconds and withdrawing slowly. Final removal of the last remnants of the CERROTRU was accomplished by etching in a concentrated HCl solution.

FOLDOUT FRAME

FOLDOUT FRAME

Table II. Summary of Cylinder Preparation and Sputter Cleaning Parameters

Run Number	Cylinder Number	Cylinder Configuration	Filler Material	Machining, Finishing Treatment, Surface Preparation, and Primary Cleaning	Sputter Cleaning Voltage, V	Current, mA	Duration, s	Pressure, N/m^2	μ
I-1	None	-	None	Lathe machined, light vapor blast, AJAX® scrub, distilled water rinse, methanol rinse	-	None	-	-	-
I-2	None	-	None	Lathe machined, heavy vapor blast, AJAX® scrub, distilled water rinse, methanol rinse	-	None	-	-	-
I-3	C-1	Fully grooved	CERROBEND®	Lathe machined, light vapor blast, AJAX® scrub, distilled water rinse, methanol rinse	-300	50	300	1.3	10
I-4	C-3	Fully grooved	CERROBEND®	Lathe machined, degreased, AJAX® scrub, distilled water rinse, methanol rinse	-450	50	300	4.5	34
I-5	C-1	Fully grooved	CERROBEND®	Lathe machined, 25% 6μ polish, 25% glass bead peen, 50% vapor blast, degrease, distilled water rinse, methanol rinse	-450	50	300	4.0	30
I-6	C-4	Quarter grooved	CERROTRU®	Lathe machined, 90% vapor blast, 10% 6μ polish, degrease, methanol rinse	-450	50	300	3.1	23
I-7	C-5	Quarter grooved	CERROTRU®	Lathe machined, vapor blast, distilled water rinse, methanol rinse	-500	50	300	3.6	27
I-8	C-9	Quarter grooved	SERMETEL® 481	Lathe machined, vapor blast, distilled water rinse, methanol rinse	None-system would not pump down due to filler outgassing				
I-9	C-7	Quarter grooved	Aluminum	Lathe machined, vapor blast, distilled water rinse, methanol rinse	-900 -600	300 300	60 60	5.5	41
I-10	C-8	Quarter grooved	Aluminum	Lathe machined, vapor blast, distilled water rinse, methanol rinse	-700 -750	300 300	60 300	3.3	25
I-11	C-4	Quarter grooved	CERROTRU®	Lathe machined, glass bead peen, distilled water rinse, methanol rinse	-700 -700	300 300	60 60	3.9	29
I-12	C-12	Quarter grooved	Aluminum	Surface ground, sanded No. 120 paper followed by No. 325 paper, vapor blast, distilled water rinse, methanol rinse	-650 -750	300 300	60 900	3.9	2.9
I-13	C-10	Quarter grooved	Aluminum	Milled lengthwise, glass bead peen, distilled water rinse, methanol rinse	-675	300	660(1)	3.9	2.9
I-14(2)	C-14	Quarter grooved	Aluminum	Milled lengthwise, vapor blast, glass bead peen, vapor blast, distilled water rinse, methanol rinse	-250	300	1620(3)	1.2	9

FOLDOUT FRAME 1

FOLDOUT FRAME 2

Table II. Summary of Cylinder Preparation and Sputter Cleaning Parameters (Continued)

Run Number	Cylinder Number	Cylinder Configuration	Filler Material	Machining, Finishing Treatment, Surface Preparation, and Primary Cleaning	Sputter Cleaning Voltage, V	Current, mA	Duration, s	Pressure, N/m^2	μ
I-15[4]	C-11	Quarter grooved	None	No machining, 25% sanded No. 600 paper, 25% vapor blast, 25% glass bead peen, 25% untreated, distilled water rinse, methanol rinse	-500	500	1200	2.2	17
I-16	C-17	Quarter grooved	Aluminum	Milled lengthwise, glass bead peen, 800°F (54 hr) vacuum bake, vapor blast, methanol soak (ultrasonic)	-800	300	960[5]	3.9	29
I-17	C-14	Quarter grooved	CERROTRU®	Milled lengthwise, 50% sanded lengthwise No. 600 paper, 50% chemical polish[6], distilled water rinse, methanol rinse	-500	60	1200	3.6	27
I-18	C-19	Quarter grooved	CERROTRU®	Milled lengthwise, sanded lengthwise No. 600 paper, ethyl alcohol rub	-500	70	840	3.6	27
I-19	C-15	Quarter grooved	Aluminum	Milled lengthwise, shot peened, dry milled lengthwise, sanded lengthwise No. 600 paper, AJAX® scrub, methanol rub, methanol rinse	-500	65	600	3.6	27
I-20	C-18	Quarter grooved	Aluminum	Dry milled lengthwise, dry machined, sanded lengthwise No. 600 paper, AJAX® scrub, methanol rub, ethyl alcohol rinse	-500	70	600	3.3	25
I-21	C-21	Fully grooved	CERROTRU®	Dry machined, sanded lengthwise No. 600 paper, AJAX® scrub, ethyl alcohol rinse	-500	70[7]	300	3.3	25
I-22	C-22	Fully grooved	Aluminum	Dry machined, sanded lengthwise No. 600 paper, AJAX® scrub, methanol rub, ethyl alcohol rinse	-500	100	1020	3.3	25
I-23	C-20	Fully grooved	CERROTRU®	Dry milled lengthwise, machined, sanded lengthwise No. 600 paper, AJAX® scrub, methanol rub, ethyl alcohol rinse	-500	55	240	3.3	25
I-24	C-22	Quarter grooved	Aluminum	Dry milled lengthwise, etched dilute HNO_3, 400°F (3 hr) vacuum bake, methanol rub	-1000	100	1200	2.7	20
I-25	C-20	Fully grooved	CERROTRU®	Dry machined, sanded lengthwise No. 600 paper, AJAX® scrub, methanol rub, ethyl alcohol rinse	-500	70	1200	3.9	29

Notes:

[1] 120 s, 240 s, and 300 s cleaning cycle with pump down between cycles

[2] Triode operation during cleaning; filament at 7.5V (108A), anode at +40V (5A)

[3] 60 s, 180 s, 600 s, 480 s, and 300 s cleaning cycle with pump down between cycles

[4] Triode operation during cleaning cycle; filament at 7V (110A), anode at +40V (7.2A)

[5] 60 s, 120 s, 180 s, 300 s and 120 s cleaning cycle with pump down between cycles + 180s target phase in cycle

[6] 1/3 HNO_3, 1/3 H_3PO_4, 1/3 CH_3COOH heated to 348°K

[7] 225 mA substrate current for first few seconds.

FOLDOUT FRAME

FOLDOUT FRAME 2

Table III. Summary of Deposition Parameters

Run Number	Cylinder Number	Cylinder Configuration	Filler Material	Substrate Voltage, V	Substrate Current, mA	Target Voltage, V	Target Current, A	Magnetic Coils Current, A	Magnetic Coils Separation, cm	Time, ks	Time, hr	Substrate Temperature, °K	Substrate Temperature, °F	Maximum Closeout Layer Thickness, mm	Maximum Closeout Layer Thickness, mils	Maximum Deposition Rate, nm/s	Maximum Deposition Rate, mil/hr	Pressure, N/m^2	Pressure, μ
								TARGET A - 10.2 cm ID											
I-1	None	--	None	Ground	-	-600	5.0	7.0	6.4	25.2	7.0	322	120	0.533	21.0	21.1	3.0	1.3	10
I-2	None	--	None	Ground	-	-530	5.1	7.7	6.4	23.4	6.5	341	155	0.584	23.0	24.9	3.5	0.9	7
I-3	C-1	Fully Grooved	CERROBEND®	-125	3	-450	4.0	7.7	6.4	7.2	2.0	336	145	0.558	22.0	30.9	4.4	1.5	11
				Ground	-	-450	4.0	7.7	6.4	10.8	3.0								
I-4	C-3	Fully Grooved	CERROBEND®	-250	5	-430	3.0	7.5	7.6	18.0	5.0	350	170	0.407	16.0	22.6	3.2	1.5	11
								TARGET B - 10.2 cm ID											
I-5	C-1	Fully Grooved	CERROBEND®	-100	65	-620	1.0	5.0	7.6	7.2	2.0	350	170	0.173	6.8	8.0	1.1	4.0	30
				-100	65	-690	1.5	6.0	7.6	7.2	2.0	358	185						
				Ground	-	-670	1.5	6.0	7.6	7.2	2.0	358	185						
I-6	C-4	Quarter Grooved	CERROTRU®	-35	6	-500	4.0	7.5	7.6	18.0	5.0	341	155	NM	NM	NM	NM	1.7	13
I-7[1]	C-5	Quarter Grooved	CERROTRU®	-50	45	-690	1.5	5.0	7.6	16.2	4.5	380	225	0.170	6.7	7.5	1.1	3.6	27
				Ground	-	-690	1.5			6.3	1.75	526	487						
I-8	C-9	Quarter Grooved	SERMETEL® 481	No deposition; system would not pump down due to filler outgassing															
I-9	C-7	Quarter Grooved	Aluminum	-200	140	-700	1.2	5.0[2]	7.6	16.2	4.5	339	151	0.142	5.6	7.5	1.1	5.3	40
				-100	140	-700	2.0	7.0	7.6	2.7	0.75	354	178					7.2	54
I-10	C-8	Quarter Grooved	Aluminum	-300	250	-725	1.8	5.0	7.6	18.9	5.25	324	124	0.173	6.8	9.1	1.3	4.5	34
I-11	C-4	Quarter Grooved	CERROTRU®	-250	215	-800	1.9	5.0	7.6	21.6	6.0	349	169	0.241	9.5	11.1	1.6	3.9	29
								TARGET C - 10.2 cm ID											
I-12[3]	C-12	Quarter Grooved	Aluminum	-250	175	-850	2.0	7.0	3.8	10.8	3.0	383	231	0.127	5.0	8.8	1.3	5.6	42
				-250	175	-1000	0.8	7.0	3.8	3.6	1.0	362	192						
								TARGET D - 11.5 cm ID											
I-13	C-10	Quarter Grooved	Aluminum	-500	250	-750	1.5	5.0	7.6	40.5	11.25	355	180	0.280	11.0	6.9	1.0	3.9	29
I-14	C-13	Quarter Grooved	Aluminum	Ground[4]	0	-500	0.8	0.0	7.6	20.7	5.75	656	722	0.231	9.1	5.1	0.8	1.1	8
				-350	120	-650	1.3	5.0	7.6	10.8	3.0		-					3.9	29
				-150	59	-650	1.3	5.0	7.6	13.5	3.75		-					3.9	29
I-15[5]	C-11	Quarter Grooved	None	Ground	0	-720	1.9	5.0	7.6	8.1	2.25	566	560	0.295	11.6	10.9	1.6	3.6	27
				-100	60	-720	1.9	5.0	7.6	7.2	2.0								
				-200	100	-720	1.9	7.5	7.6	7.2	2.0								
				-200	194	-750	4.4	7.5	7.6	0.9	0.25								
				-100	84	-750	4.4	7.5	7.6	3.6	1.0								
I-16	C-17	Quarter Grooved	Aluminum	-500	140	-500	1.0	5.0	7.6	1.8	0.5	482	408	0.580	22.8	12.9	1.8	3.9	29
				-250	60	-570	1.4	5.0	7.6	2.7	0.75								
				-250	89	-670	2.0	5.0	7.6	14.4	4.0								
				-250	89	-650	2.0	5.0	7.6	9.7	2.75								
				-150	89	-650	4.8	7.5	7.6	16.2	4.5								
I-17	C-14	Quarter Grooved	CERROTRU®	-500	86	-450	1.0	5.0	7.6	14.4	4.0	364	195	0.052	2.0	3.6	0.5	3.6	27
				-250	75	-615	2.0	5.0	7.6	14.4	4.0			0.129	5.1	9.0	1.3		
				-100	84	-905	4.0	5.0	7.6	22.5	6.25			0.493	19.4	21.9	3.1		

2 FOLDOUT FRAME

Table III. Summary of Deposition Parameters (Continued)

Run Number	Cylinder Number	Cylinder Configuration	Filler Material	Substrate Voltage, V	Substrate Current, mA	Target Voltage, V	Target Current, A	Magnetic Coils Current, A	Magnetic Coils Separation, cm	Time, ks	Time, hr	Substrate Temperature, °K	Substrate Temperature, °F	Maximum Closeout Layer Thickness, mm	Maximum Closeout Layer Thickness, mils	Maximum Deposition Rate, nm/s	Maximum Deposition Rate, mil/hr	Pressure, N/m^2	Pressure, μ
								TARGET E - 11.7 cm ID											
I-18	C-19	Quarter Grooved	CERROTRU®	-500	60	-470	0.5	5.0	7.6	14.4	4.0		NM	0.021	0.8	1.5	0.2	3.3	25
				-500	60	-450	0.5	5.0	7.6	15.3	4.25			0.024	0.9	1.6	0.2		
				-500	90	-615	1.0	5.0	7.6	19.8	5.50			0.078	3.1	4.0	0.6		
				-500	155	-800	3.0	7.0	7.6	6.3	1.75			0.099	3.9	15.7	2.2		
				-0.6	73	-730	3.0	7.0	7.6	2.7	0.75			0.037	1.4	13.7	1.9		
				-25	18	-760	4.0	7.5	7.6	26.1	7.25			0.550	21.6	21.1	3.0		
I-19	C-15	Quarter Grooved	Aluminum	-500	70	-450	0.7	5.0	7.6	1.8	0.5		NM	0.003	0.1	1.7	0.2	3.2	24
				-250	42	-450	0.8	5.0	7.6	5.4	1.5			0.013	0.5	2.4	0.4		
				-250	40	-450	0.8	5.0	7.6	18.0	5.0			0.083	3.3	4.6	0.7		
				-250	50	-600	1.1	5.0	7.6	9.0	2.5			0.021	0.8	2.3	0.3		
				-250	53	-600	1.1	5.0	7.6	4.5	1.25			0.024	0.9	5.3	0.8		
				-100	63	-1000	2.0	5.0	7.6	21.6	6.0			0.238	9.4	11.0	1.6		
I-20	C-18	Quarter Grooved	Aluminum	-500	70	-450	0.7	5.0	7.6	21.6	6.0		NM	0.074	2.9	3.4	0.5	3.3	25
				-250	54	-600	1.1	5.0	7.6	48.5	13.5			0.249	9.8	5.1	0.7		
				-100	65	-1000	2.1	5.0	7.6	28.8	8.0			0.025	1.0	0.9	0.1		
I-21	C-21	Fully Grooved	CERROTRU®	-500	75	-450	0.9	5.0	7.6	27.9	7.75			0.056	2.2	2.0	0.3	3.3	25
				-500	80	-500	1.1	5.0	7.6	46.7	13.0			0.191	7.5	4.1	0.6		
				-500	160	-1000	2.4	5.0	7.6	27.9	7.75			0.332	13.1	11.9	1.7		
I-22	C-22	Fully Grooved	Aluminum	-50	0	-350	0.9	6.5	7.6	19.8	5.5			0.038	1.5	1.9	0.3	3.3	25
				-50	0	-250	0.9	6.5	7.6	3.6	1.0			-	-	-	-		
				-25	10	-600	4.2	6.5	7.6	20.7	5.75			0.356	14.0	17.2	2.4		
I-23	C-20	Fully Grooved	CERROTRU®	-500	65	-350	0.7	5.0	7.6	13.5	3.75		NM	0.017	0.7	1.3	0.2	3.3	25
				-500	60	-350	0.5	5.0	7.6	18.0	5.0			0.020	0.8	1.1	0.2	3.3	25
				-500	80	-450	1.2	5.0	7.6	18.0	5.0			0.068	2.7	3.7	0.5	3.3	25
				-500	100	-550	1.8	5.2	7.6	43.2	12.0			0.284	11.2	6.7	0.9	3.3	25
				-500	155	-800	3.3	5.0	7.6	7.2	2.0			0.101	4.0	14.0	2.0	3.3	25
				-500	140	-1000	2.0	4.0	7.6	9.0	2.5			0.094	3.7	10.4	1.5	1.6	12
				-25	21	-1000	2.3	4.0	7.6	7.2	2.0			0.094	3.7	13.1	1.9	1.6	12
				-25	25	-1000	5.0	5.0	7.6	3.6	1.0			0.094	3.7	26.1	3.7	1.6	12
				-250	90	-1000	5.0	4.8	7.6	3.6	1.0			0.091	3.7	26.1	3.7	1.6	12
I-24[6]	C-16	Quarter Grooved	Aluminum	-500	140	-800	4.0	4.7	7.6	5.4	1.5		NM	0.292	11.5	20.6	2.9	2.7	20
				-25	21	-1000	4.0	4.1	7.6	1.8	0.5							2.7	20
				0	0	-1000	3.4	4.5	7.6	7.2	2.0							0.7	5
				0	0	-1000	2.5	4.5	7.6	4.5	1.25			0.420	16.5	16.7	2.4	0.7	5
				0	0	-800	3.5	7.5	7.6	11.7	3.25							0.5	4
				0	0	-700	4.5	8.0	7.6	9.0	2.5							0.5	4
								TARGET F - 11.7 cm ID											
I-25	C-23	Fully Grooved	CERROTRU®	-900	50	-400	0.6	5.0	7.6	18.0	5.0		NM	1.015	40.0	10.7	1.4	3.6	29
				-400	84	-550	1.1	5.0	7.6	9.0	2.5							3.3	25
				0	0	-700	1.0	5.0	7.6	5.4	1.5							1.6	12
				0	0	-1000	1.7	5.0	7.6	37.8	10.5							1.6	12
				0	0	-1000	3.2	6.0	7.6	30.6	8.5							1.6	12

NOTES:

(1) Operated in triode mode last 1.75 hr

(2) For first hour of operation, 5A coil current was used

(3) Discharge unstable during entire run

(4) Triode operation with filament at 8.5 v (115a) and anode at +40v (15a) for first 5.75 hr

(5) Filament operated without anode to heat substrate throughout run

(6) After 5.5 hr, system evacuated, 5 min back sputter 1000 v (230 mA) at 25μ pressure

NM - Not Measured

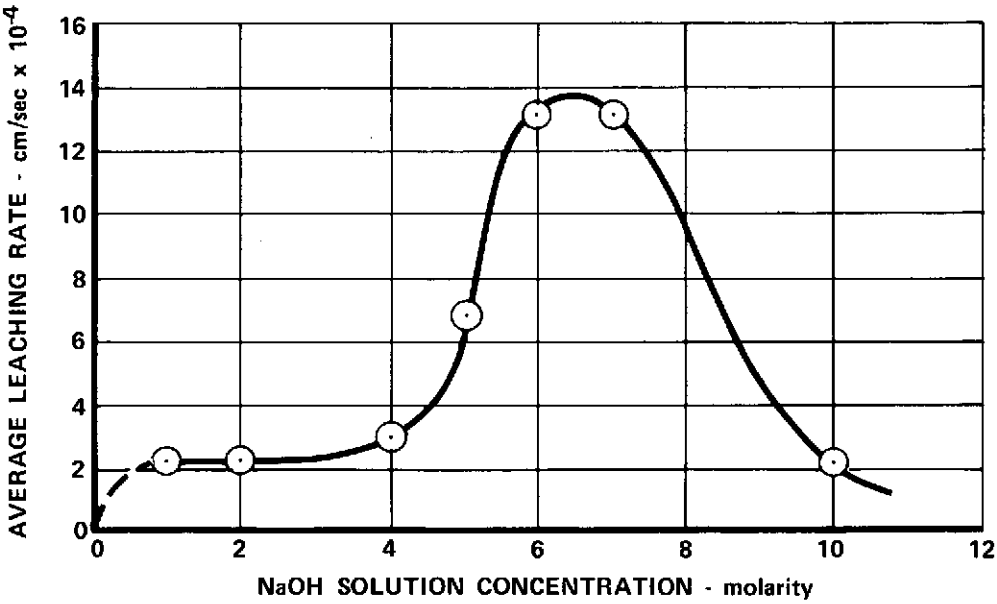

Figure 6. Effect of NaOH Solution Molarity on the Average Leaching Rate of the Flame-Sprayed Aluminum Filler of Ambient Temperatures FD 78193

RESULTS AND DISCUSSION

The closeout layer thickness was measured throughout the program to evaluate the geometrical characteristics of the selected sputtering configuration and to determine if thickness distribution was changing as a result of nonuniform target depletion. Typically, the circumferential distribution at the cylinder center varied between ±5% of the average coating thickness. (See figure 7.) This variation in coating thickness was attributed to deviations from perfect symmetry of the target, substrate, and magnetic field during deposition. The longitudinal closeout layer thickness distributions obtained in all runs were typical of those shown in figure 8. The basic shape of the distribution over the cylinder length was a consequence of the similar length of substrate (12.7 cm) and target (14.6 cm). The change in longitudinal distribution with deposition was attributed to the change in target geometry due to the nonuniform sputter removal of material. Similar distribution profiles with a similar type device have been previously observed and described by Gill and Kay. [8]

The distributions obtained were acceptable for the filler material evaluation to be performed since the required deposit thickness was relatively small. Where thicker deposits would be required longer targets or modification of the target ends would have to be performed. The various filler materials, processing techniques and deposition parameters are discussed separately in the following sections.

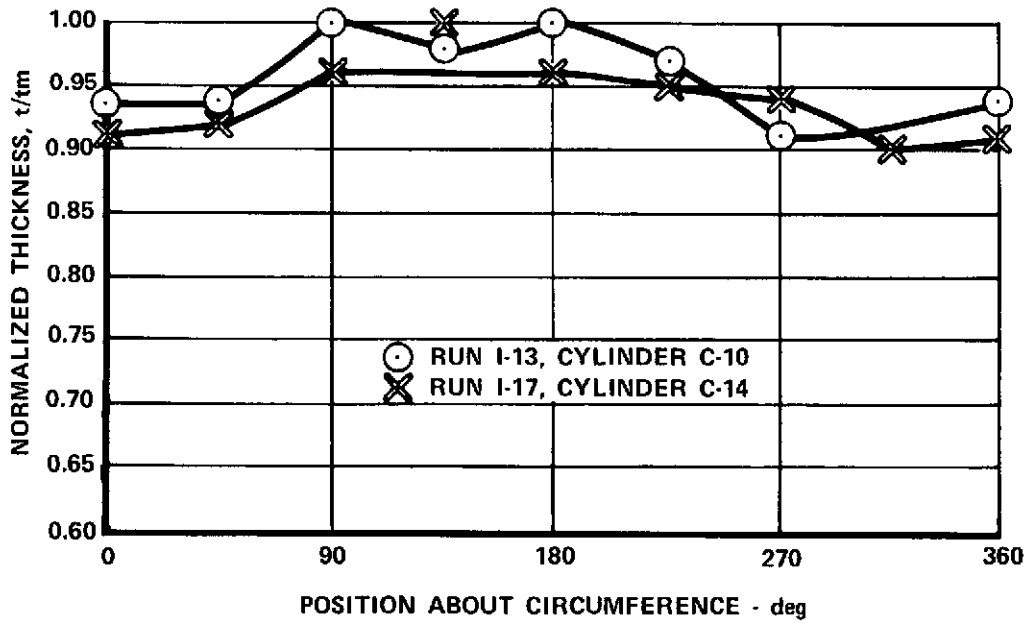

Figure 7. Circumferential Closeout Layer Thickness Distribution at Cylinder Center FD 78481

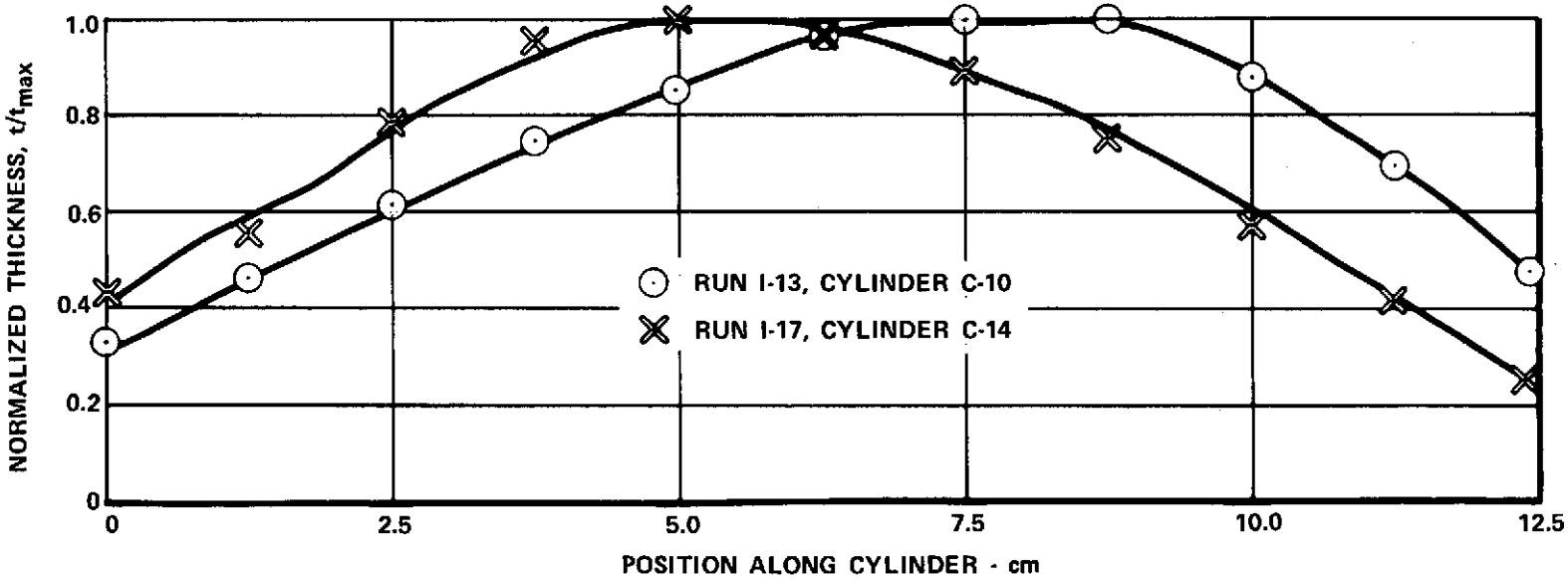

Figure 8. Closeout Layer Thickness Distribution Along Cylinder Length FD 78482

Effects of Filler Materials

Of the filler materials evaluated, CERROCAST, CERROBEND, and SERMETEL 481 were found to be unacceptable for use in the fabrication of thrust chambers by sputtering. The high shrinkage characteristics of CERROCAST resulted in incomplete filling of the grooves after repeated filling attempts. The casting technique being used with the low melting alloys would require modification to allow for the shrinkage of the CERROCAST. Application of this filler in contoured thrust chambers would be extremely difficult. Although, the casting of CERROBEND into the grooves resulted in adequate filling, this use of this filler resulted in severe bond contamination. The closeout layer removed from the rib lands of run I-3 exhibited discoloration indicative of CERROBEND contamination. This was qualitatively identified by spark source emission spectrography to contain Cd, Bi, Sn, and Pb, the constituents of CERROBEND. Bond contamination also resulted in the cylinders produced in runs I-4 and I-5. The SERMETEL 481 filler was found to be unacceptable due to continuous outgassing in the vacuum environment. Without using the high temperature curing cycle (3.6 ks at 813°K) which would anneal the OFHC copper substrate, the SERMETEL 481 was porous and contained entrapped gases that prevented acceptable vacuum levels to be obtained. Furthermore, the surface could not be densified sufficiently to yield a smooth surface.

Aluminum was found to be the most suitable filler for thrust chamber fabrication. However, the method of application by flame-spraying was found to be unacceptable. The application by flame-spraying resulted in a porous structure (figure 9), which exhibited extensive outgassing. System contamination was undoubtably the most excessive in the experiments in which this filler material was used. A direct result of the contamination was the oxide layer at the bond interface observed in runs I-14 and I-16. Whether the oxide layer formed entirely during the sputter cleaning, the in-site bakeout cycles, or the initial stages of the deposition cycle could not be determined from the experiments performed.

Of the filler materials investigated, aluminum was the most easily removed and provided the highest bond strengths. The investigation of other techniques for applying the aluminum filler, such as vapor deposition, ion plating, or sputtering, was beyond the scope of this program.

The CERROTRU filler was used in eight of the experimental depositions, with some measure of success. Contamination of the interface between the closeout layer and the rib surfaces resulted in lowering the bond strength. The degree to which the interface was contaminated seemed to depend on the severity and duration of the sputter cleaning operation. A technique for the application of CERROTRU was developed that provided a complete filling of the grooves. Removal of the last remnants of the CERROTRU was usually accomplished by etching in a concentrated HCl solution. This procedure sometimes resulted in embrittling the closeout layer. The embrittlement was attributed to the openness of the closeout layer.

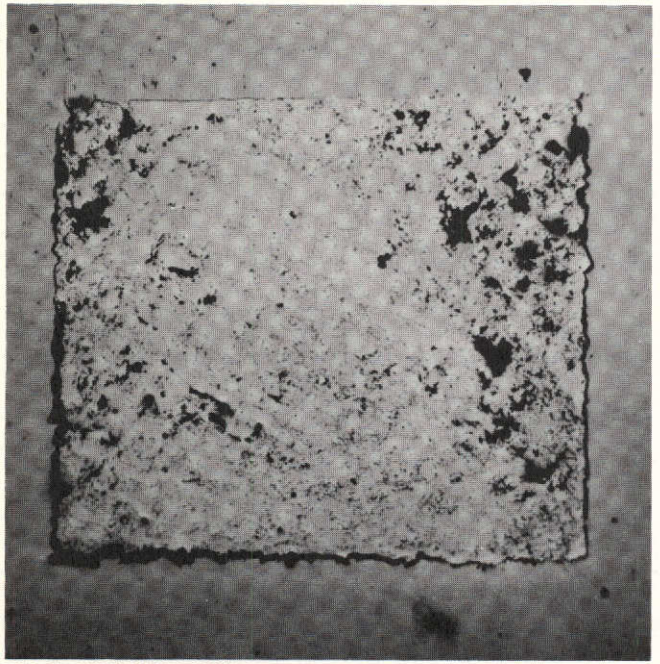

MAG: 88X UNETCHED

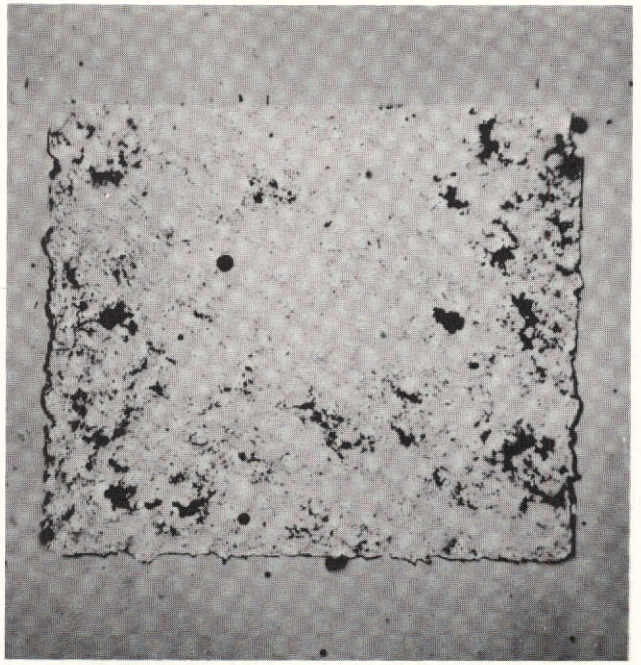

MAG: 88X ETCHED

Figure 9. Typical Appearance of Aluminum Filler

FD 78491

Effects of Predeposition Processing

From the initial depositions performed on cylinders prepared by normal lathe machining techniques, it was observed that this method of machining tended to smear the filler and substrate and result in the formation of a large burr on one side of the rib edge. On the nonburred side of the rib edge, the filler material was pulled away from the rib wall. The sputtered closeout layer persistently exhibited cracks extending from the nonburred side of the groove. (See figure 10.) Longitudinal surface grinding was evaluated in run I-12 as a means of forming burrs on both sides of the grooves. The grinding technique introduced deep machining marks into substrate, which required excessive sanding for removal. Longitudinal milling did not result in deep machining marks, but did yield significant burring along both sides of the grooves. As is apparent in figure 11, burring the groove sides did not in itself eliminate the cracking problem, although a reduction in severity of the cracking was noted.

Suspecting that the machining lubricants trapped in the filler material during milling also contributed to the crack formation through the introduction of contaminants, dry milling was used in run I-19. Though the outgassing rate of the aluminum filler was significantly reduced, the cracking problem persisted. Dry machining using a reversing cutting technique resulted in minimal cracking at the rib wall and reduced the extent of cracking in the closeout layer. (See figure 12.)

Concurrent with the variations in machining, surface deformation techniques such as glass bead peening and shot peening were also tried as a means of further sealing the incipient cracks at the rib walls and, in the case of the flame-sprayed aluminum filler, densifying the surface layer to decrease outgassing and seal the surface porosity. Though these techniques resulted in further decreasing the cracking frequency and severity, the problem was not totally eliminated. (See figures 13 and 14.) Other techniques, such as vacuum baking prior to installation in the sputtering chamber (runs I-16 and I-24), radiation heating of the sample at high vacuum in the sputtering chamber for 54 ks (15 hr) (runs I-17 and I-18), and multiple sputter clean-pumpdown cycles (runs I-13, I-14, and I-16), were used to reduce filler outgassing and crack formation. Though these techniques were successful in reducing the filler outgassing, the cracking problem persisted.

The effects of the different surface treatments on the presence of defects in the closeout layer were initially deduced from the comparison of the structures of the closeout layers on the filled copper substrates from several runs. However, the effect of surface finish was usually overshadowed by other effects, attributable to the filler material, deposition parameters, etc. The glass bead peening operation seemed to contribute most to the interfacial contamination on the copper substrates (figure 15) and promote defect formation. To further confirm this, a separate deposition similar to I-14 was performed on an aluminum substrate prepared with three different surface finishes (glass bead peened, vapor blasted, and sanded with 600-grit SiC paper) on different areas of the cylindrical substrate. It was again observed that the glass bead peening operation promoted the formation of defects in the coating. (See figure 16.) The defects were normal to the surface and traced back to the centers of the concave regions of the surface.

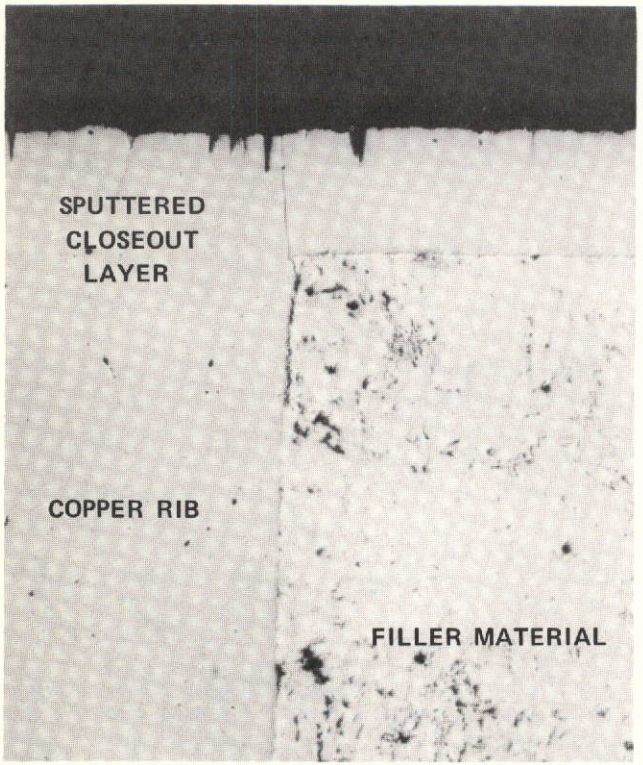

MAG: 100X UNETCHED

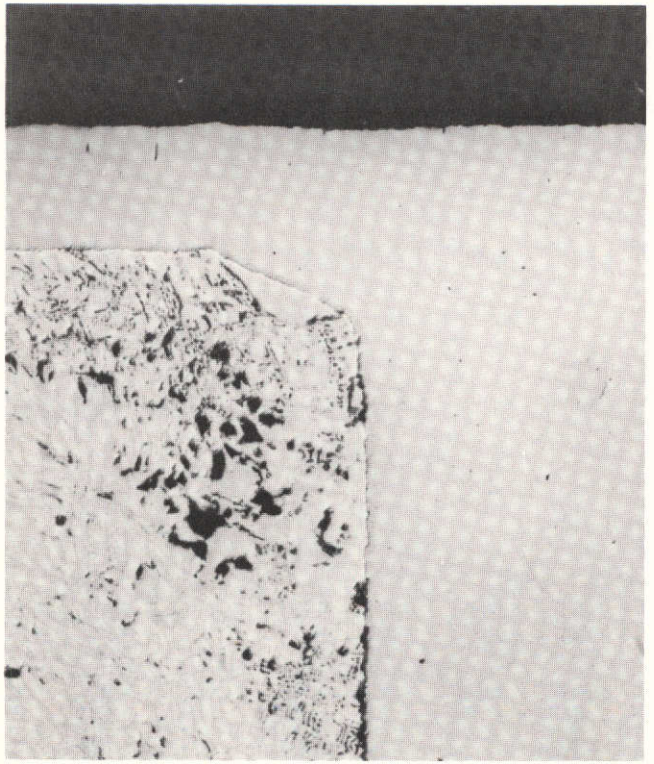

MAG: 100X UNETCHED

Figure 10. Burring and Closeout Layer Cracking Resulting from Normal Lathe Machining, Run I-7 FD 78485

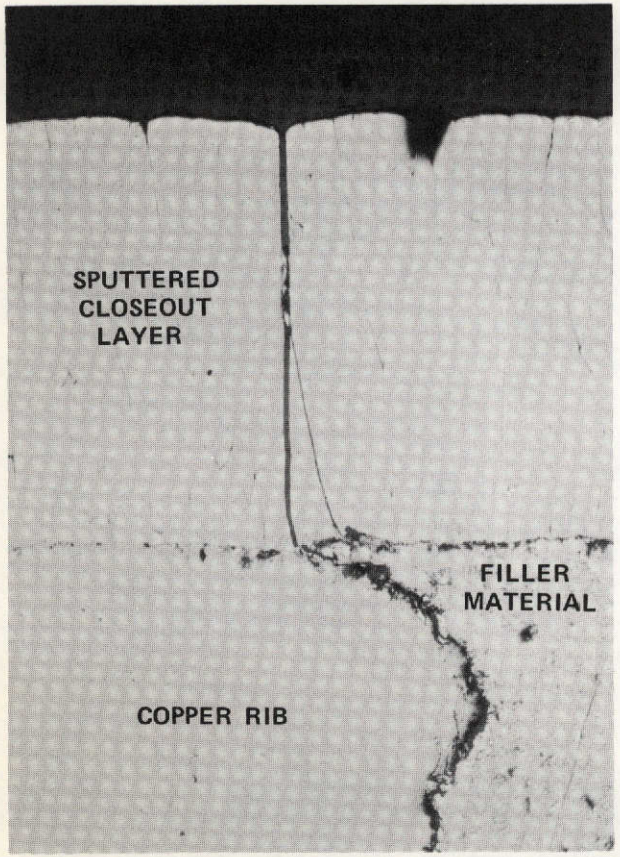

Figure 11. Burring and Closeout Layer Cracking Resulting from Lengthwise Milling, Run I-16

FD 78486

Figure 12. Appearance of Closeout Layer on Dry Machined and Sanded Substrate, Run I-20

FD 78487

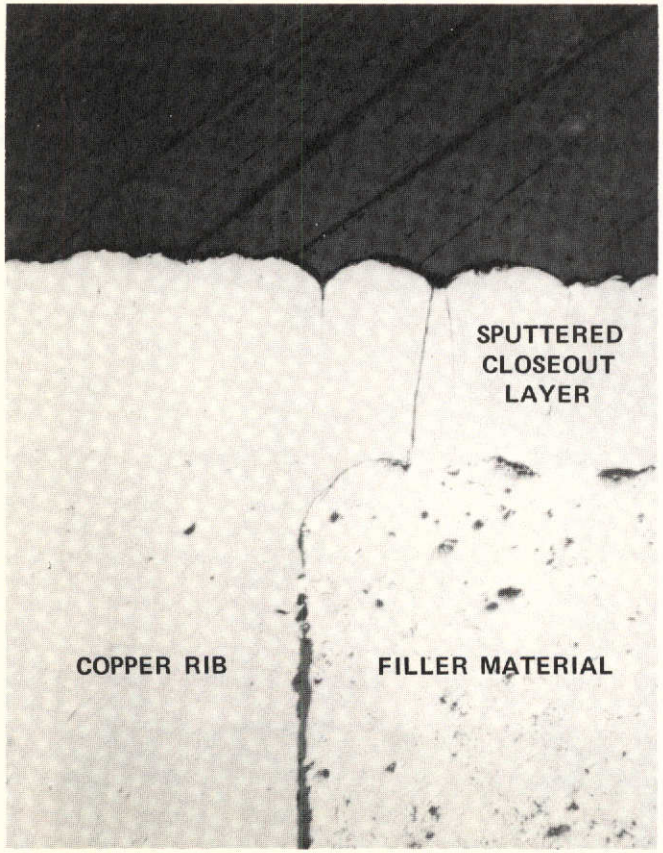

MAG: 100X UNETCHED

Figure 13. Cracking of Closeout Layer on Glass-Bead-Peened Surface, Run I-13 FD 78488

MAG: 250X UNETCHED

Figure 14. Cracking of Closeout Layer on Shot-Peened and Dry Milled Surface, Run I-19 FD 78489

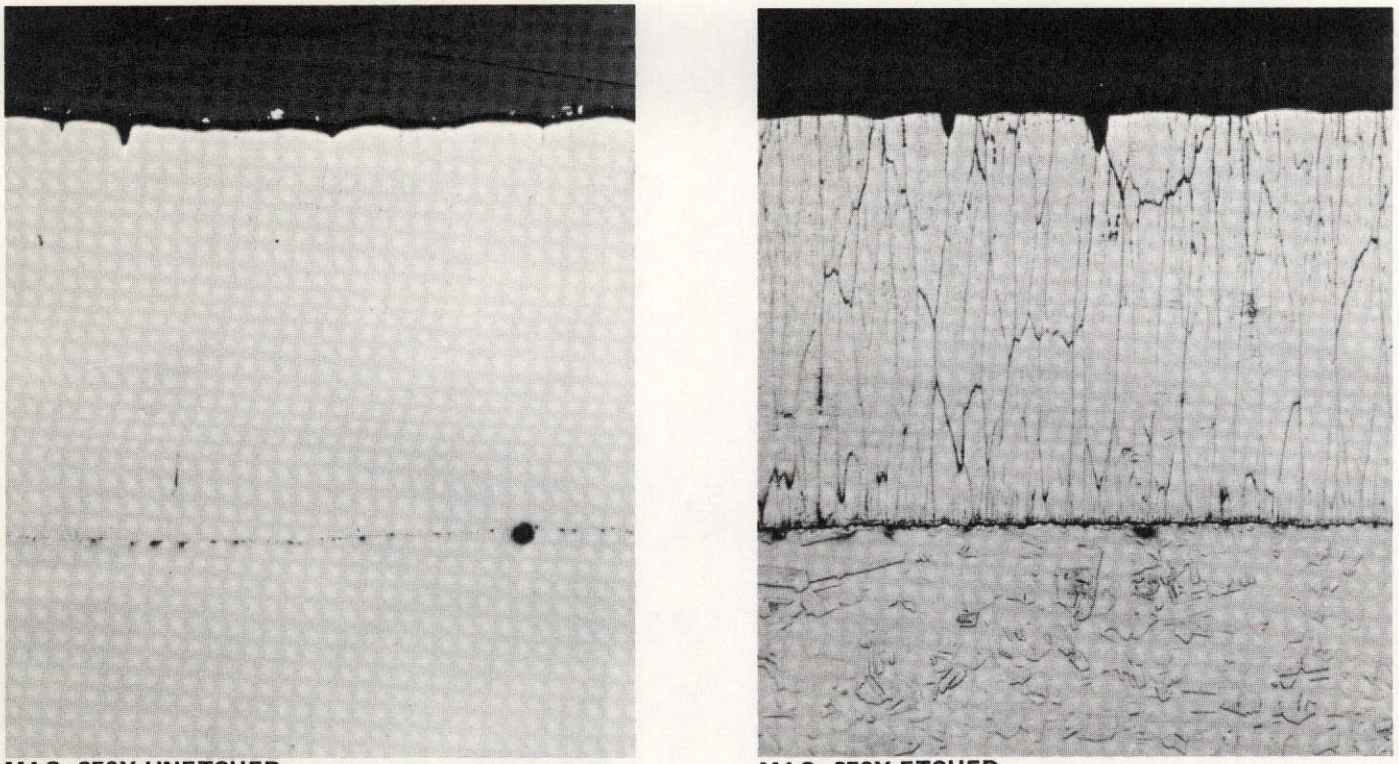

MAG: 250X UNETCHED

MAG: 250X ETCHED

Figure 15. Interfacial Contamination Resulting from Glass Bead Peening, Run I-16

FD 78492

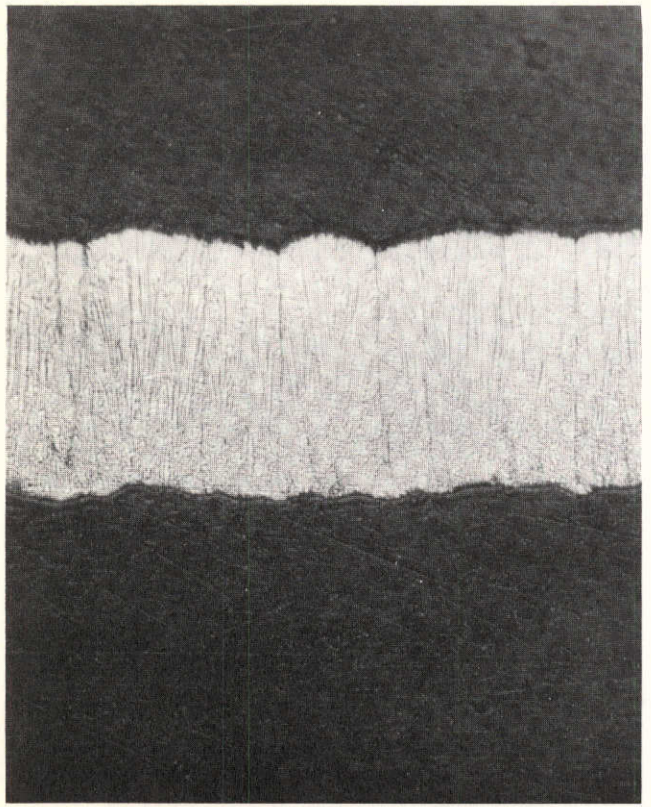

MAG: 250X SUBSTRATE REMOVED, ETCHED

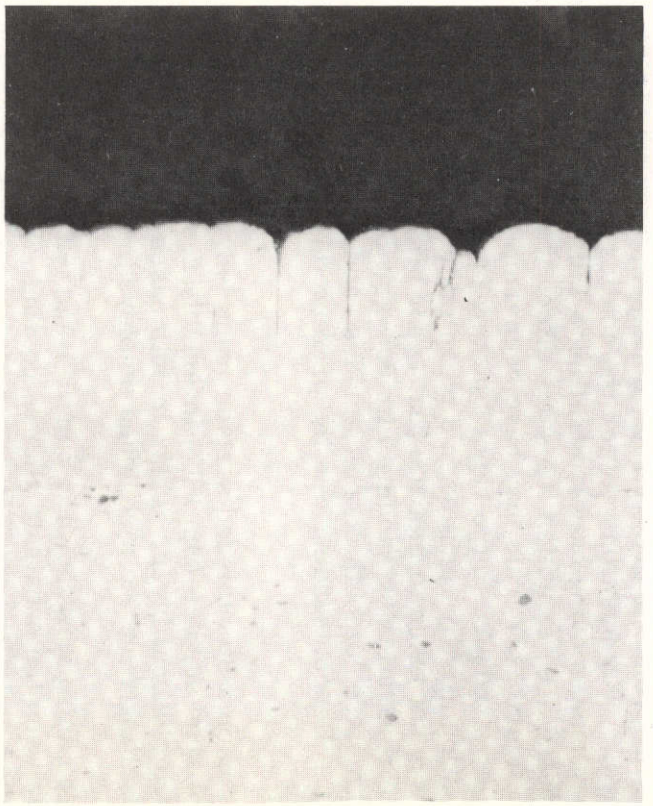

MAG: 250X UNETCHED

Figure 16. Microstructure of Sputtered OFHC Copper on Glass-Bead-Peened Region of Type 6061 Aluminum Alloy Substrate

FD 78494

The defects probably resulted because of the deposition rate difference between the concave regions and the convex regions. The concave regions exhibited a lower growth rate since these areas were exposed to a smaller segment of the cylindrical target (shadowing effect) than the convex regions. As the deposition continued, the difference in growth rate increased, resulting in deeper and deeper "valleys." The junction between the coating on adjacent "hills" eventually became a sharp cusp moving outward trailing a thin crack or open boundary. The vapor-blasted area exhibited the same effect, but with fewer resultant defects. (See figure 17.) This may have been due, in part, to the contamination at the interface, attributed to the vapor blasting process. It should be noted that vapor blasting usually resulted in a clean interface, (figure 18), so that the above result was not taken to indicate that vapor blasting should be discontinued. However, the preparation by sanding with 600-grit SiC paper resulted in a defect-free structure, smooth deposit surface, and a high quality interface. (See figure 19.) Hence, sanding was the preferred preparation technique for the latter runs.

Deposition on a 6μ polished surface (runs I-5, I-6, and I-15) and on a chemically polished surface (run I-17) invariably resulted in poorer adherence of the sputtered closeout layer. This, in both cases, was attributed to contamination resulting from the techniques employed.

Sputter cleaning was shown in runs I-1 and I-2 to be essential in obtaining a good bond between the substrate and the coating. Variations in sputter cleaning procedure were tried with each filler material examined. (See table II.) The determination of the optimum sputter cleaning procedure was for the most part empirical, being based on the relative difficulty of mechanically removing the sputtered layer.

In tensile testing the closeout layers on cylinders C-15 and C-18 (aluminum filler), failure stresses of 63.6 and 72.3 MN/m^2 (9,230 and 10,500 psi) were attained. (See table IV.) Yielding of the rib would be expected to occur at about 45,000 psi. The above failures occurred by pulling closeout layer material from between the ribs. (See figure 20.) The closeout layer was not removed from the rib surfaces. This type of fracture was attributed to the presence of cracks in the closeout layer that resulted during deposition. Since material was not removed from the rib areas, a bond strength could not be determined. A similar failure also occurred at 67.6 MN/m^2 (9,800 psi) with the sample tested from cylinder C-19 (CERROTRU filler). The sample from cylinder C-21 (CERROTRU filler) exhibited a 0.69 MN/m^2 (100 psi) bond strength, and all of the closeout layer was removed. This extremely low bond strength was attributed to overheating in the initial sputter cleaning, which resulted in substantial interface contamination. A similar failure, however, at a higher stress, 10.6 MN/m^2 (1540 psi) was exhibited by the sample from cylinder C-20 (CERROTRU filler). (See figure 21.) With this sample, the low bond strength was probably due to inadequate sputter cleaning, since a 240-second cleaning cycle was employed as compared to an 840-second cycle for cylinder C-19.

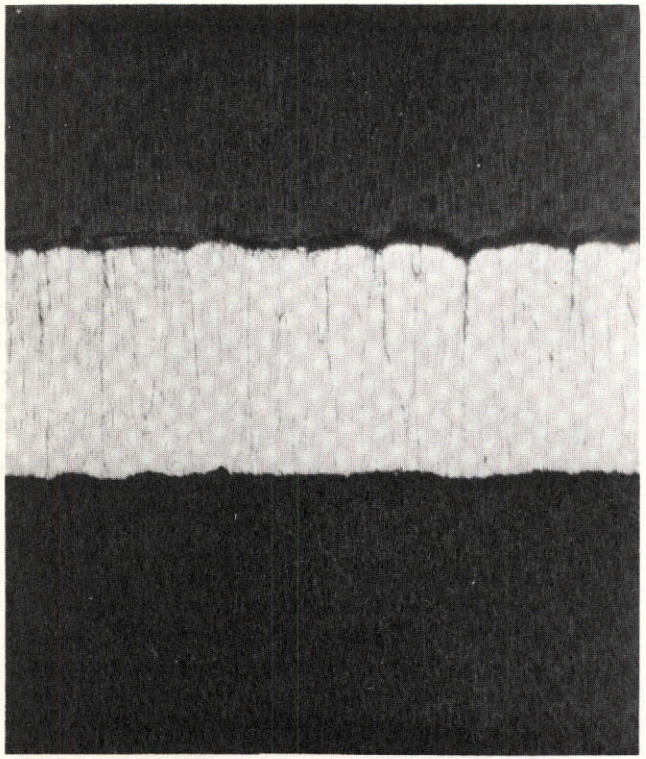

MAG: 250X SUBSTRATE REMOVED, ETCHED

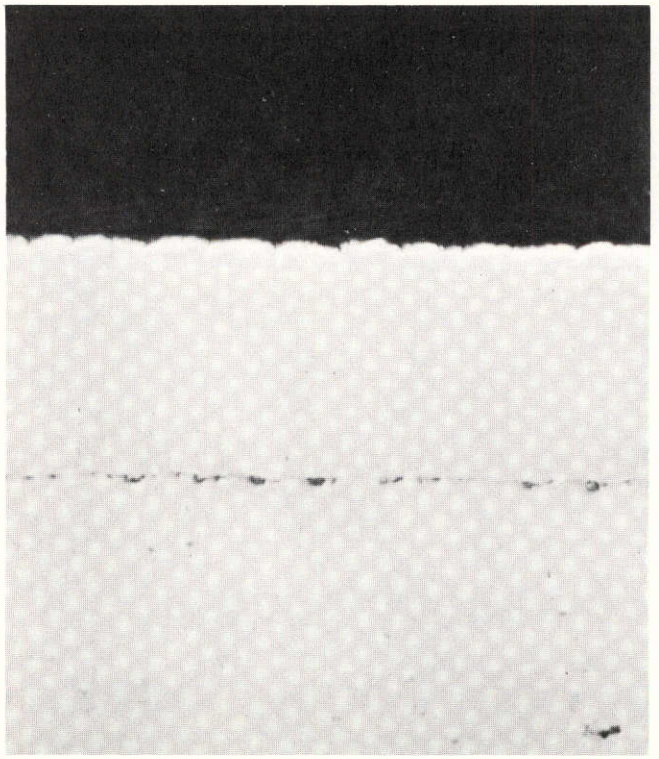

MAG: 250X UNETCHED

Figure 17. Microstructure of Sputtered OFHC Copper on Vapor-Blasted Region of Type 6061 Aluminum Alloy Substrate FD 78496

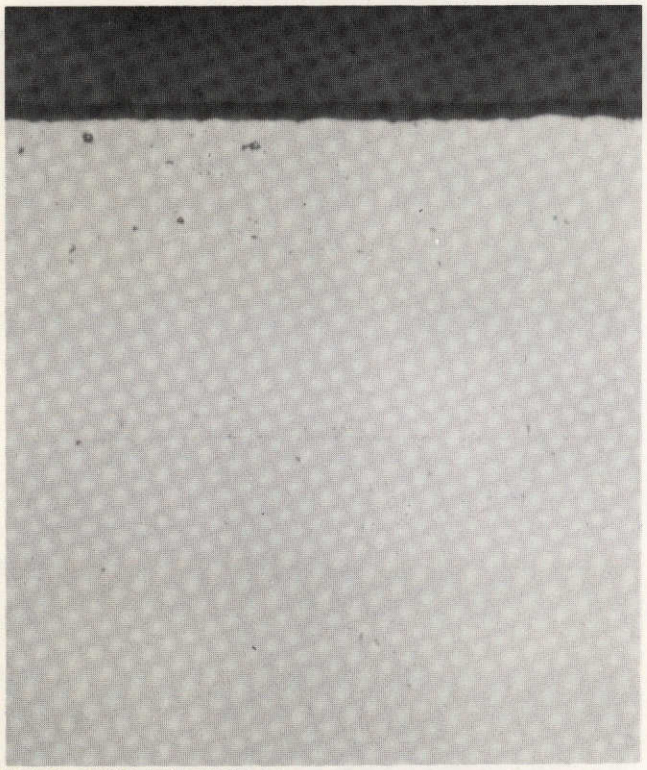

MAG: 250X UNETCHED

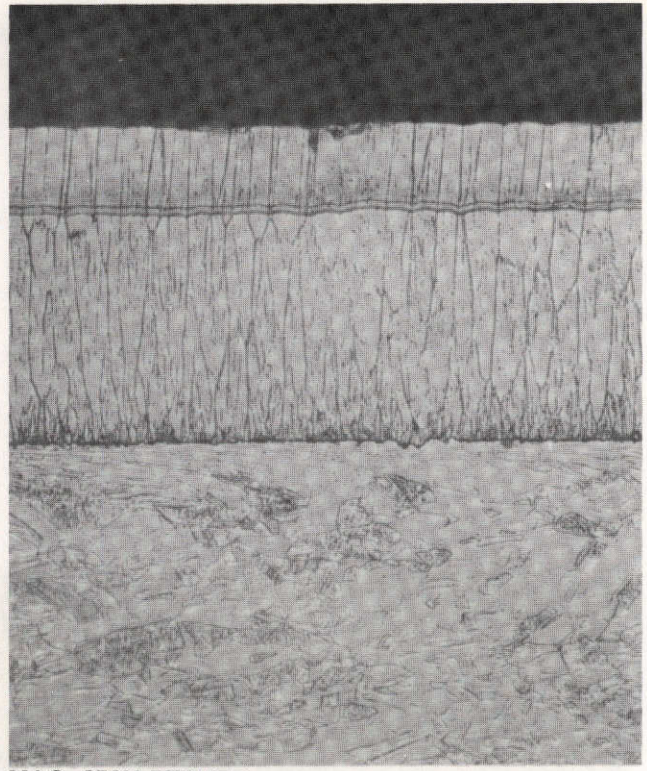

MAG: 250X ETCHED

Figure 18. Typical Clean Interface Between Closeout Layer and Substrate Obtained Using Vapor Blasting as Final Surface Preparation, Run I-7

FD 78493

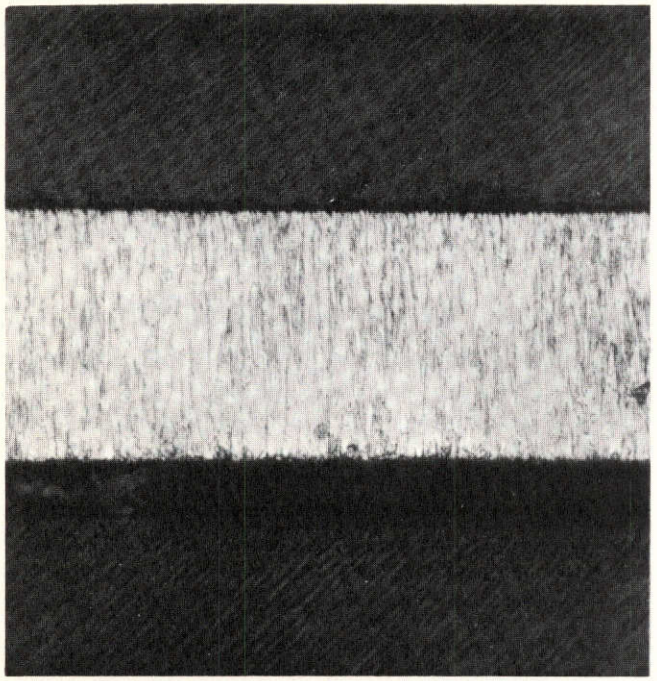

MAG: 250X SUBSTRATE REMOVED, ETCHED

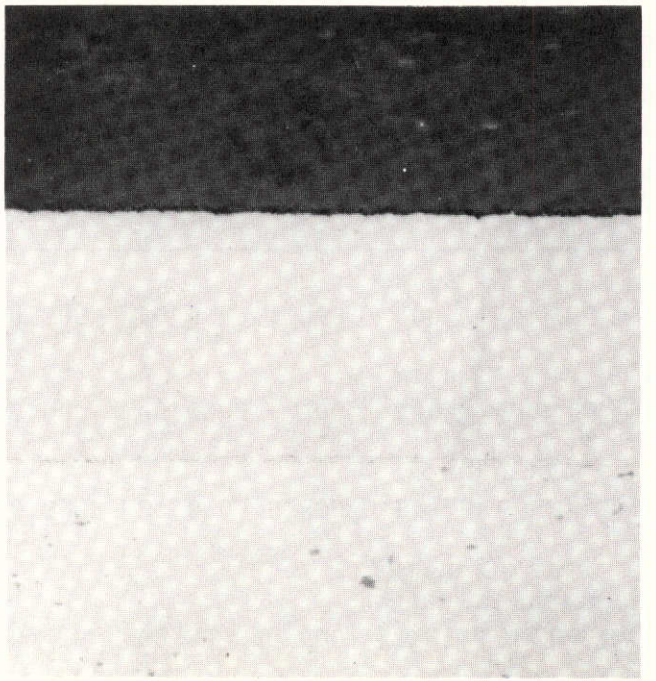

MAG: 250X UNETCHED

Figure 19. Microstructure of Sputtered OFHC Copper on 600-Grit-Sanded Region of Type 6061 Aluminum Alloy Substrate

FD 78495

Table IV. Results of Room Temperature Tensile Testing

Run	Cylinder	Filler	Tensile Load, N	Tensile Load, lb	Area, $m^2 \times 10^{-4}$	Area, in^2	Tensile Stress, MN/m^2	Tensile Stress, psi	Remarks
I-19	C-15	Aluminum	21,350	4,800	3.35	0.520	63.6	9,230	Failure in coating between ribs; no material removed from rib area.
I-20	C-18	Aluminum	21,306	4,790	2.93	0.455	72.3	10,500	Failure in coating between ribs; no material removed from rib area.
I-18	C-19	CERROTRU®	22,685	5,100	3.35	0.520	67.6	9,800	54% of coating removed from rib area.
I-21	C-21	CERROTRU®	222	50	3.23	0.500	0.69	100	100% removed from rib area.
I-23	C-20	CERROTRU®	2,091	470	1.97	0.305	10.6	1,540	100% removed from rib area.

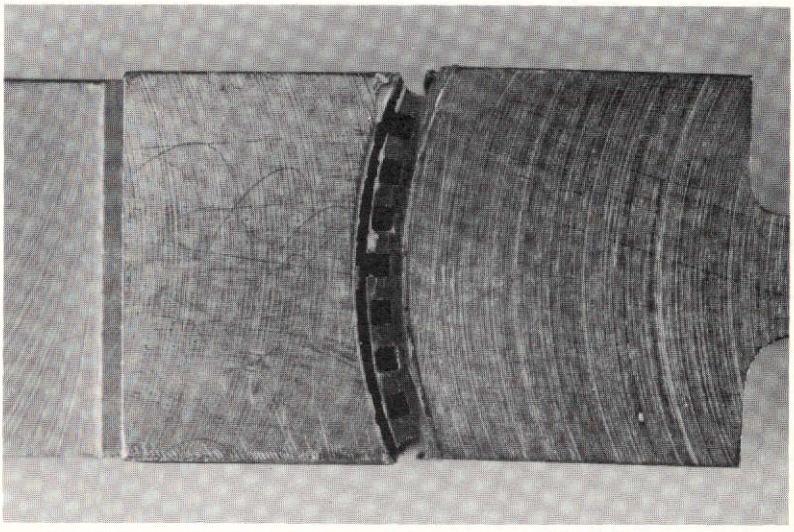

A. CYLINDER C-15 FROM RUN I-19 FAL 30486

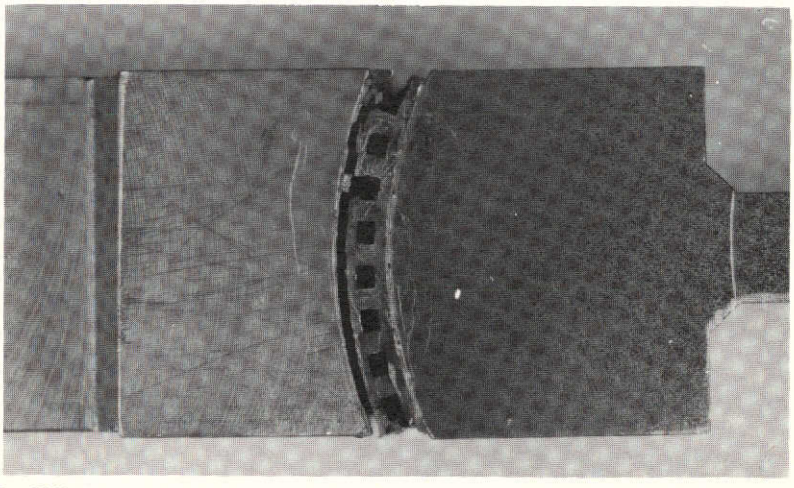

B. CYLINDER C-18 FROM RUN I-20 FAL 30537

Figure 20. Appearance of Closeout Layer Fracture After Room Temperature Tensile Testing of Segments from Aluminum-Filled Cylinders C-15 and C-18 FD 78183

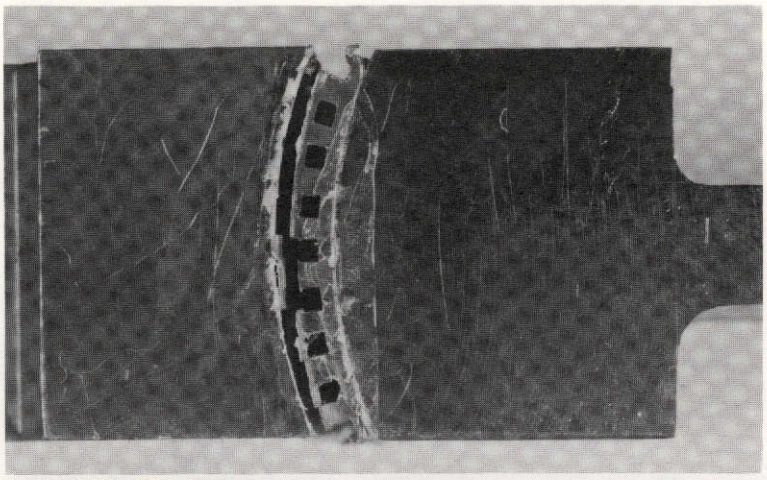

A. CYLINDER C-19 FROM RUN I-18 FAL 30488

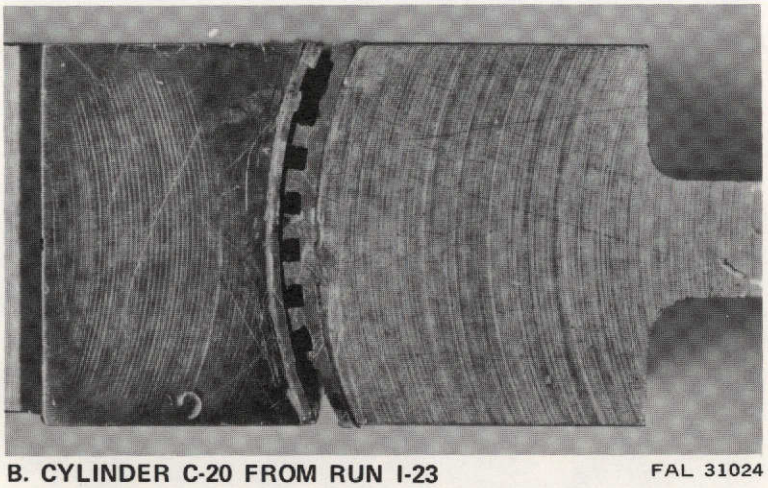

B. CYLINDER C-20 FROM RUN I-23 FAL 31024

Figure 21. Appearance of Closeout Layer Fracture After Room Temperature Tensile Testing of Segments from CERROTRU®-Filled Cylinders C-19 and C-20 FD 78191

On the closeout layer removed from the rib lands in tensile testing of the three CERROTRU filled samples (C-19, C-20, and C-21) a visual discoloration was observed on the underside of the deposit. Quantitative chemical analysis of the closeout layer from cylinders C-19 and C-21 showed minimal quantities of filler elements. (See table V.) The surface contamination resulting with CERROTRU may represent a contamination level beyond the detectable limits of normal chemical analysis. The results of the chemical analysis on the deposit removed from aluminum filled cylinder C-18 showed minimal aluminum contamination. Apparently, if aluminum is present at the interface, its presence results in less degradation of bond strength than does the presence of the CERROTRU material.

Table V. Chemical Analysis of Sputtered Closeout Layer

Run	Cylinder	Filler	Bi	Sn	Kr(*)	Al
I-17	C-14	CERROTRU®	0.5 ppm	2 ppm	1040 ppm	0.2 ppm
I-20	C-18	Aluminum	<0.5 ppm	2 ppm	1800 ppm	2 ppm
I-18	C-19	CERROTRU®	0.5 ppm	2 ppm	2300 ppm	1 ppm
I-20	C-21	CERROTRU®	0.5 ppm	2 ppm	7300 ppm	0.2 ppm

*Krypton analysis performed by Pyrolysis Gas Chromatography; all others by Spark Source Mass Spectrography.

Effects of Deposition Parameters

The initial depositions performed in this program were directed at the use of high-rate sputter deposition at 21.1 to 35.3 nm/s (3.0 to 5.0 mils/hr) to form the closeout layer. The structure that resulted was filled with defects (cones, open boundaries, cracks). A typical cone is shown in figure 22. When the rate was decreased to 7.1 to 14.1 nm/s (1.0 to 2.0 mils/hr), the defects were generally reduced in number and severity. Variations in substrate bias and deposition temperature were employed along with variations in filler material, machining, and cleaning techniques in an attempt to eliminate the structural defects of the sputtered closeout layer. Since all of the processing and coating parameters were not to be systematically investigated in this program, the selection of the deposition parameters was usually based on the results of the previous experiments. The consequence of using this procedure to select the parameters was a limitation of the degree to which the effect of a given variable could be ascertained. However, certain trends were noted to correspond with the results of other investigators.

The effect of deposition temperature on coating structure generally correlated well with that observed by Thornton.[9] The depositions performed at T/T_m = 0.2 to 0.3 (271 to 406°K) exhibited columnar grains. (See figure 23.) The depositions performed at T/T_m = 0.3 to 0.5 (406 to 678°K) exhibited a more equiaxed structure and, for the highest temperatures in this T/T_m range, showed indications of concurrent recrystallization. (See figure 24.) As was expected, the temperature of deposition affected the hardness of both the closeout layer and the substrate, (figure 25 and table VI). The scatter in the closeout layer hardness at low temperatures was attributed to the openness of many of the low temperature deposits. (See figure 26.)

Since it was believed that outgassing of the filler material might be contributing to the formation of cracks in the closeout layer, low rate initial depositions were employed to minimize the filler material heating and subsequent outgassing. If the low rate deposition was followed by a high rate deposition not exceeding about 14.1 nm/s (2.0 mils/hr), the closeout layer was usually quite free of open defects. (See figures 27 and 28.)

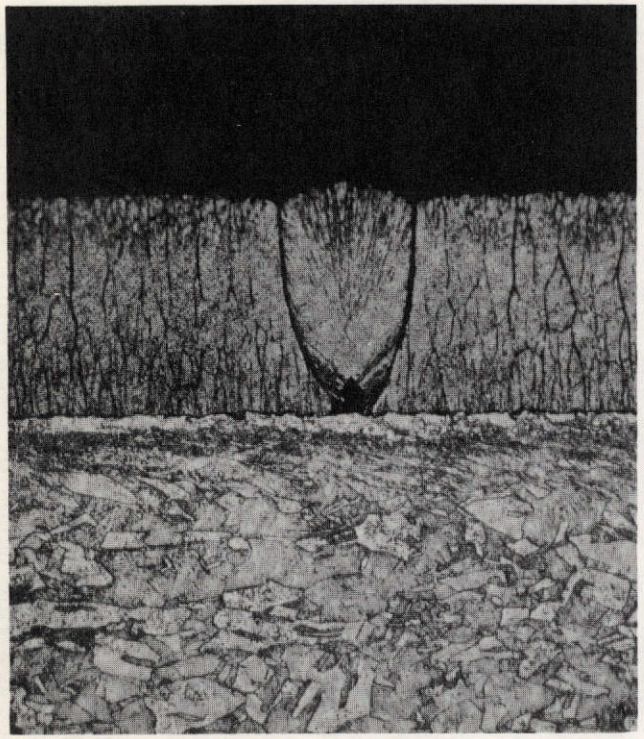

MAG: 250X ETCHED

Figure 22. Appearance of Cone in OFHC Copper Closeout Layer, Run I-17

FD 78747

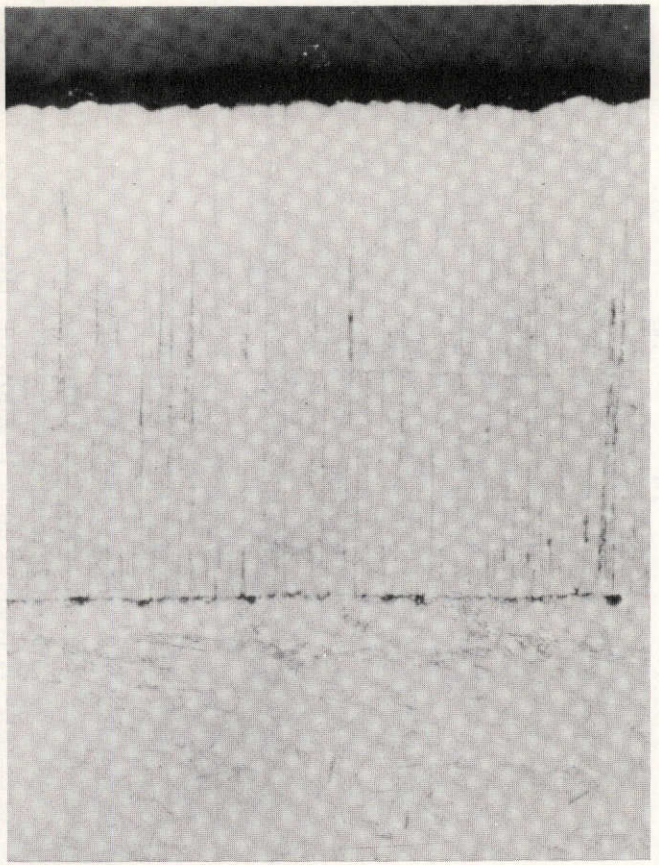

MAG: 250X

Figure 23. Columnar Grain Structure Sputtered OFHC Copper Applied at a Substrate Temperature of 355°K (82°C), Run I-18

FD 78497

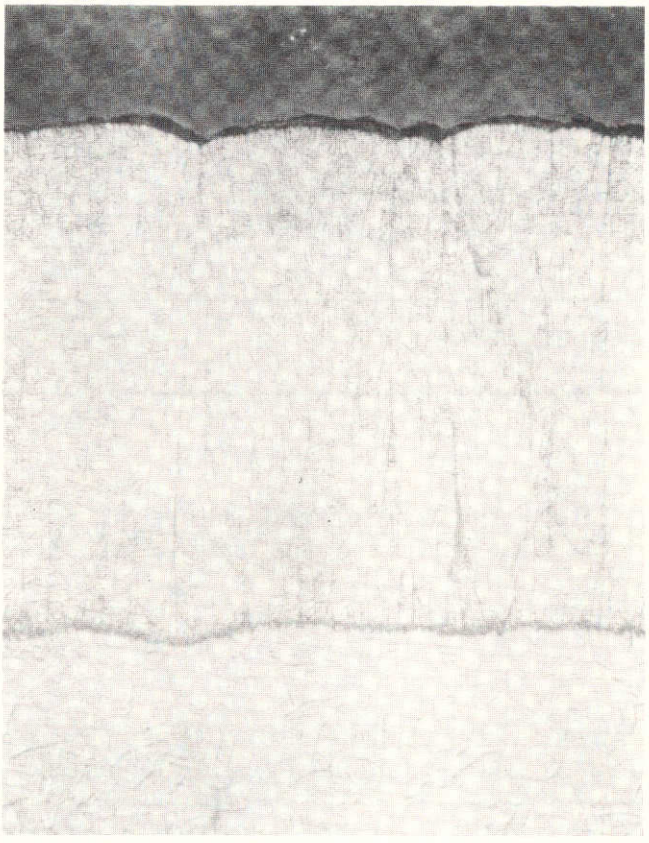

MAG: 250X ETCHED

Figure 24. Microstructure of Sputtered OFHC Copper Applied at a Substrate Temperature of 566°K (293°C), Run I-15 FD 78498

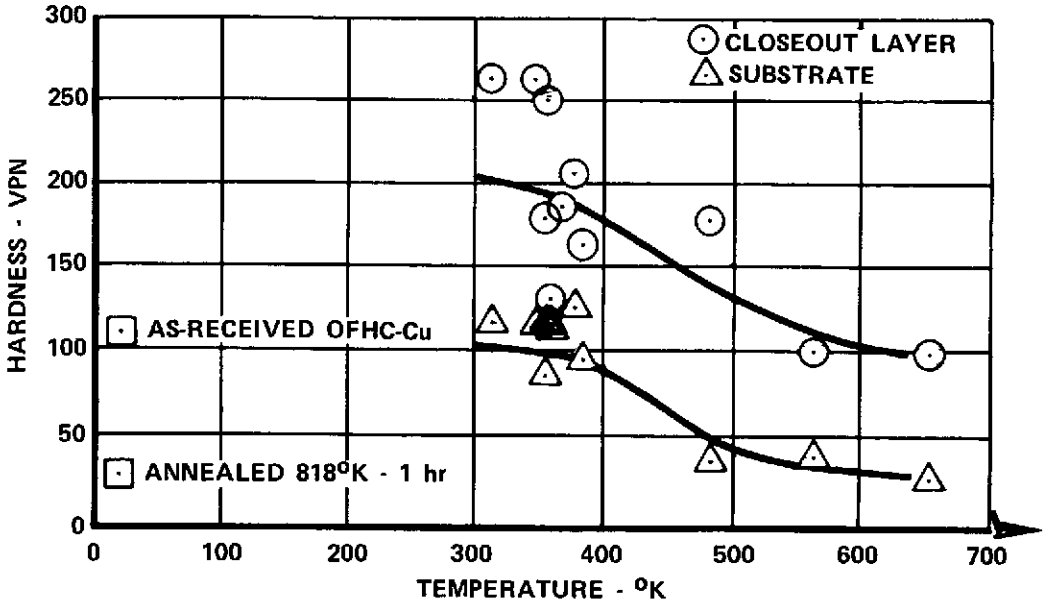

Figure 25. Effect of Substrate Temperature on Closeout Layer and Substrate Hardness

FD 78483

Table VI. Hardness of Sputtered OFHC Copper Coatings and Substrates (0.2-kg Load, Diamond Pyramid Indenter)

Run Number	Cylinder Number	Coating Hardness (VPN)	Substrate Hardness (VPN)	Deposition Temperature (°K)
I-5	C-1	227	112	358
I-7	C-5	207	110	380
I-9	C-7	178	114	354
I-10	C-8	256	114	324
I-11	C-4	256	111	349
I-12	C-12	161	91	382
I-13	C-10	225	83	355
I-14	C-13	96	25	656
I-15	C-11	99	38	566
I-16	C-17	175	36	482
I-17	C-14	181	123	364
I-18	C-19	247	114	NM*
I-19	C-15	191	123	NM
I-20	C-18	247	129	NM
I-21	C-21	231	139	NM
I-22	C-22	79	123	NM
I-23	C-20	195	121	NM
I-24	C-16	183	127	NM

NM - Not measured

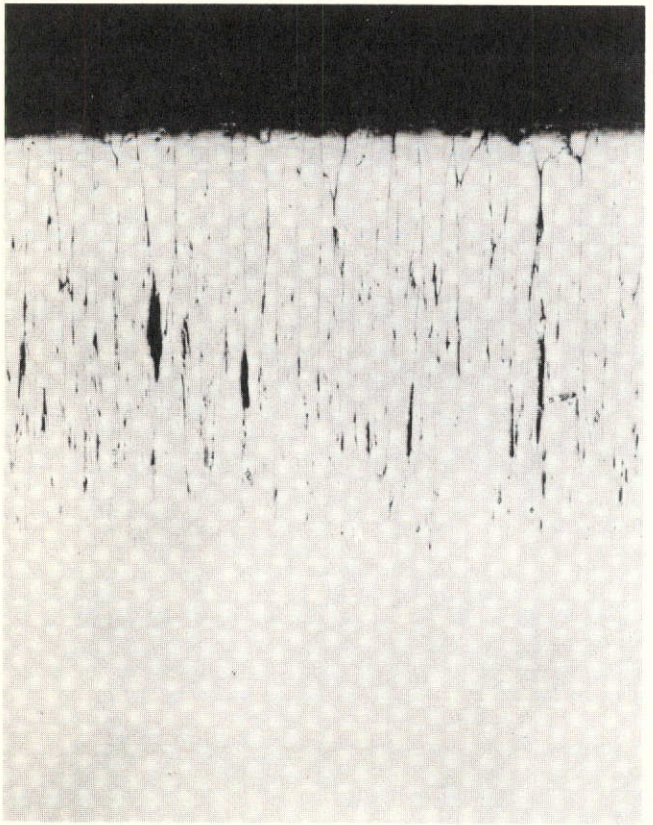

MAG: 100X UNETCHED

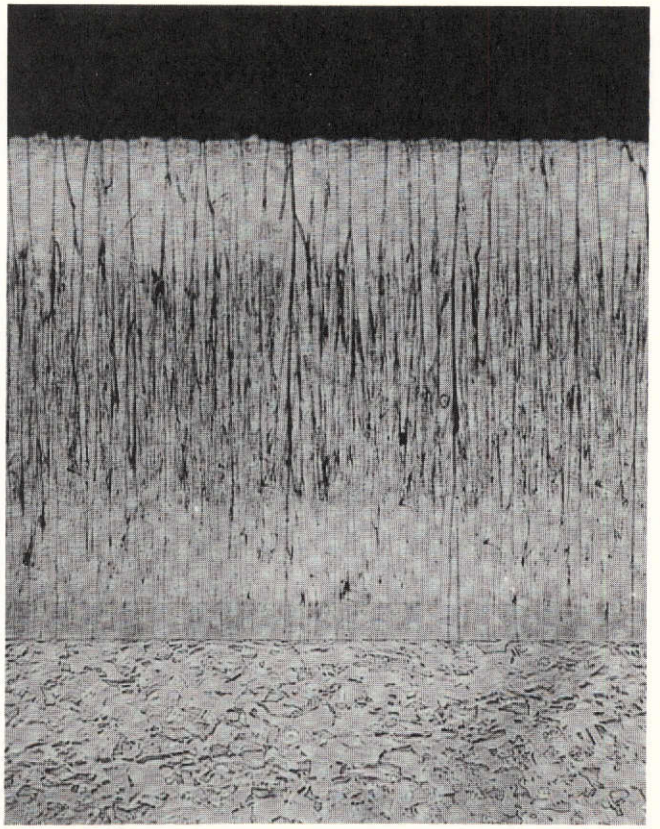

MAG: 100X ETCHED

Figure 26. Open Microstructure of Closeout Layer Applied Using High Rate and Low Temperature, Run I-17 FD 78499

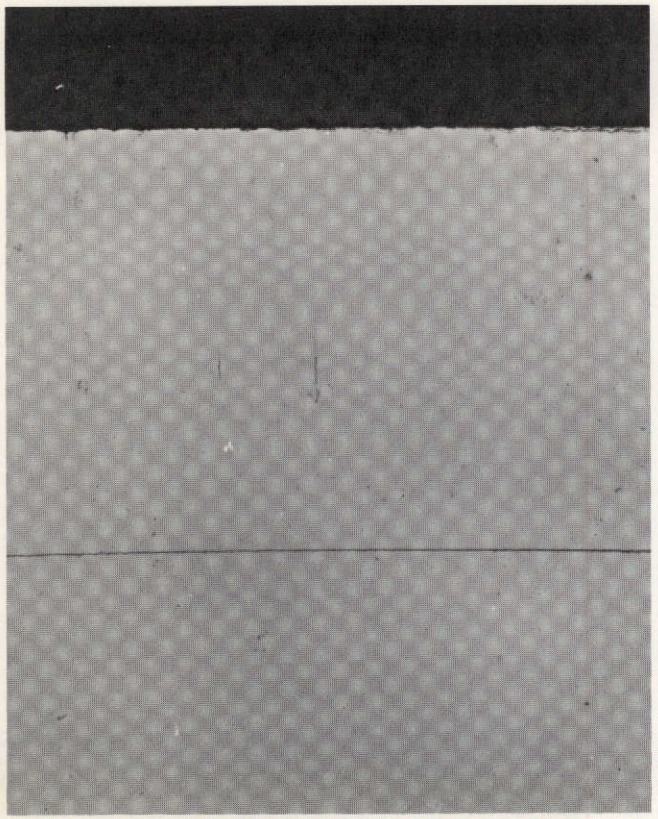

MAG: 100X UNETCHED

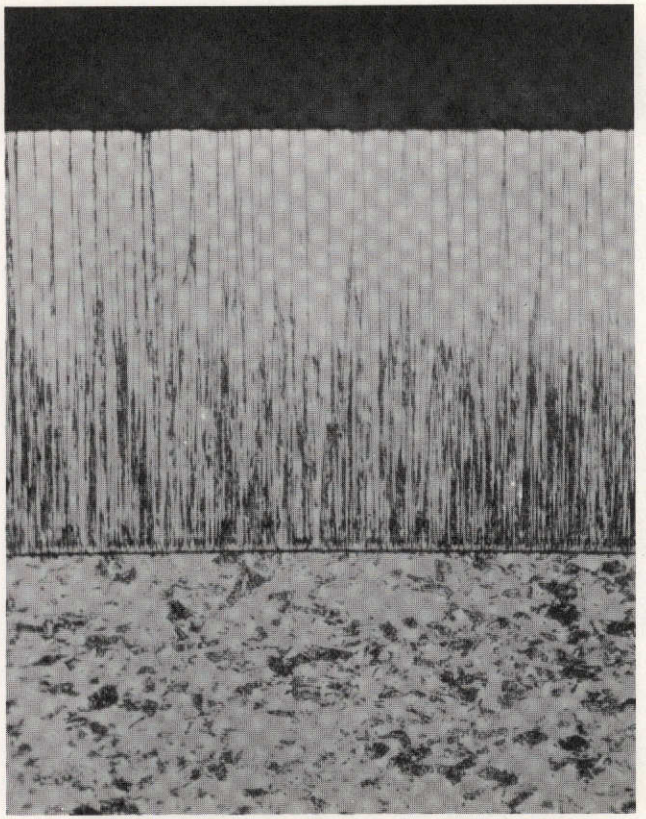

MAG: 100X ETCHED

Figure 27. Microstructure of Closeout Layer Applied Using Low Rate Initial Deposition Followed by a High Rate Deposition at Less Than 14.1 nm/s (2.0 mils/hr), Run I-21

FD 78500

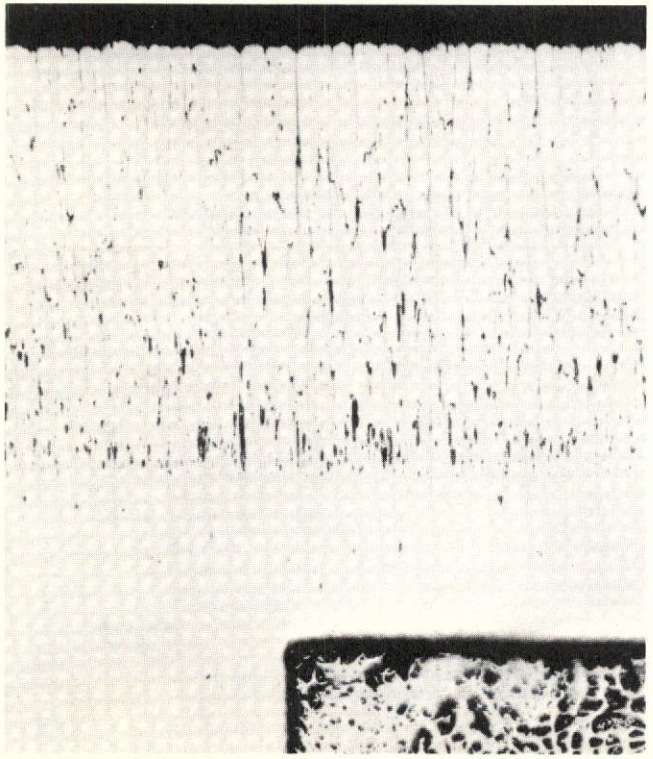

MAG: 100X UNETCHED

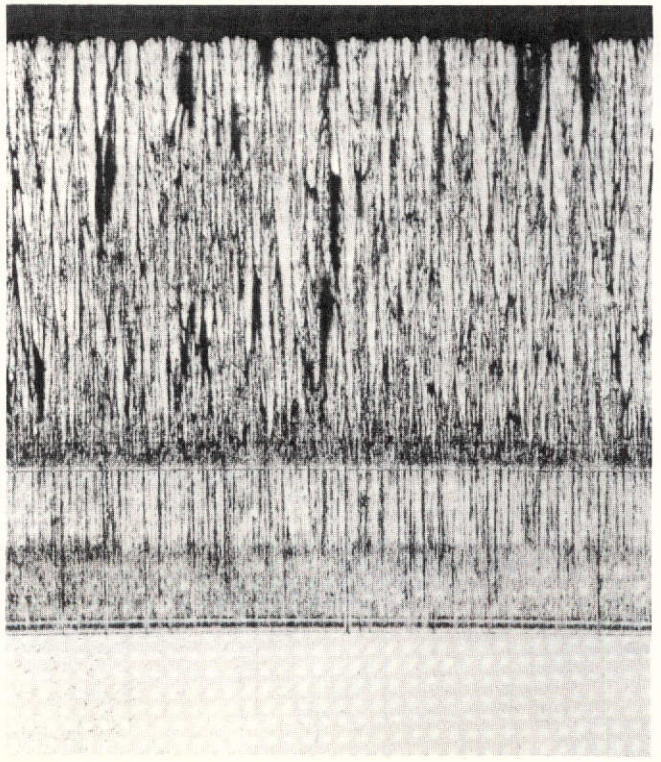

MAG: 100X ETCHED

Figure 28. Microstructure of Closeout Layer Applied Using Low Rate Initial Deposition, Followed by High Rate Depositions at More Than 14.1 nm/s (2.0 mils/hr), Run I-18 FD 78743

The bias on the substrate was varied to determine its effect on cone formation and closeout layer structure. The competing effects of substrate surface finish, filler material outgassing, deposition rate, and temperature made it impossible to single out the effect of substrate bias on structure and cone formation. However, bias was found to affect the level of sputtering gas entrapment. (See table V.) The amount of krypton in the samples seemed to correlate well with the percentage of the deposit applied with a substrate bias of -500V. (See figure 29.)

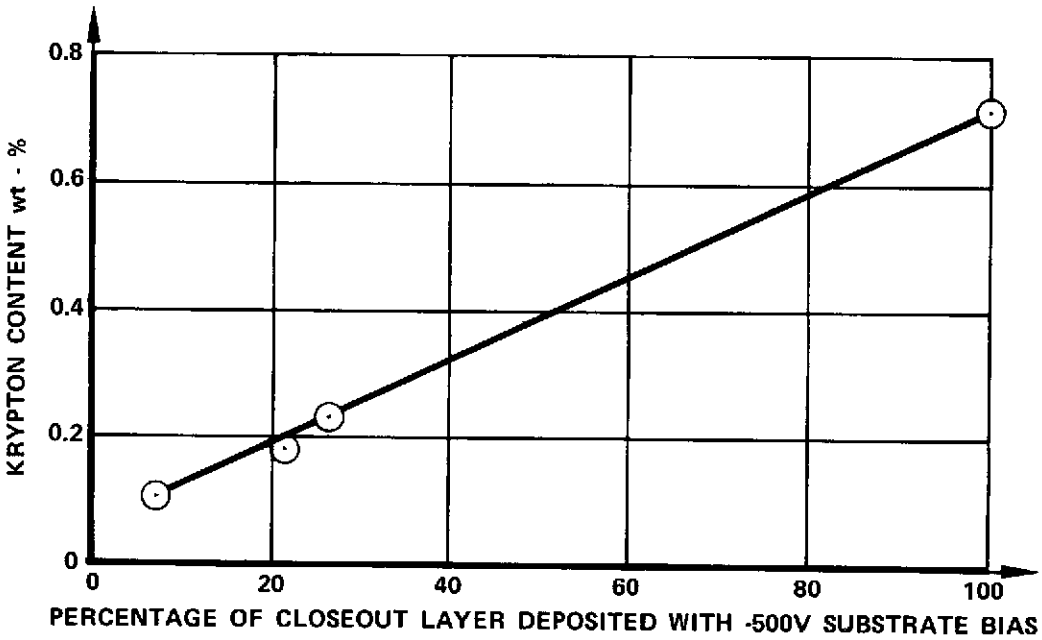

Figure 29. Effect of Bias on Krypton Content FD 78480

Based on the results of Thornton, [9] lowering the sputtering gas pressure should permit the use of higher deposition rates without obtaining the characteristic open structures at the low deposition temperatures required by the OFHC copper substrates and/or the low melting point filler materials. Although the one run (I-24) performed with a lower discharge pressure did yield a closeout layer with fewer defects (figure 30), the improvement in quality could not be attributed solely to the lower pressure since several of the other parameters were also changed.

Final Cylinder Fabrication

Based on the results of the previous depositions and evaluations, a final cylinder representative of a regeneratively cooled thrust chamber was fabricated in run I-25. (See tables II and III and figure 31.) The initial layers were deposited at about 4 nm/s (0.6 mils/hr) to avoid filler heatup and to bridge the filler with a heat conductive layer. The remaining deposition was performed at a slightly higher rate, approximately 14.1 nm/s (2.0 mil/hr). The applied closeout layer thickness was approximately 0.102 cm in the center and 0.051 cm on the ends.

MAG: 200X UNETCHED

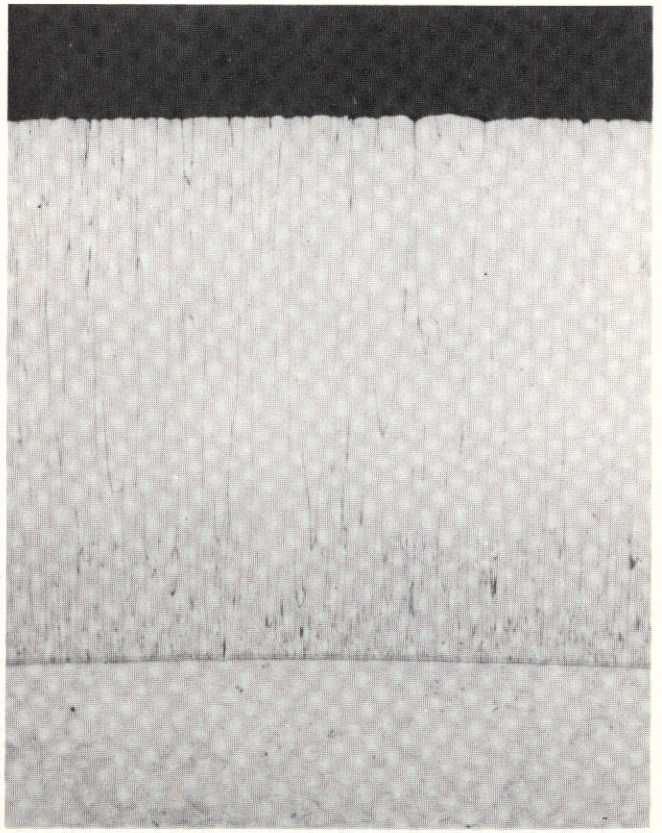

MAG: 200X ETCHED

Figure 30. Microstructure of Closeout Layer Applied Using Lower Discharge Pressure, Run I-24 FD 78745

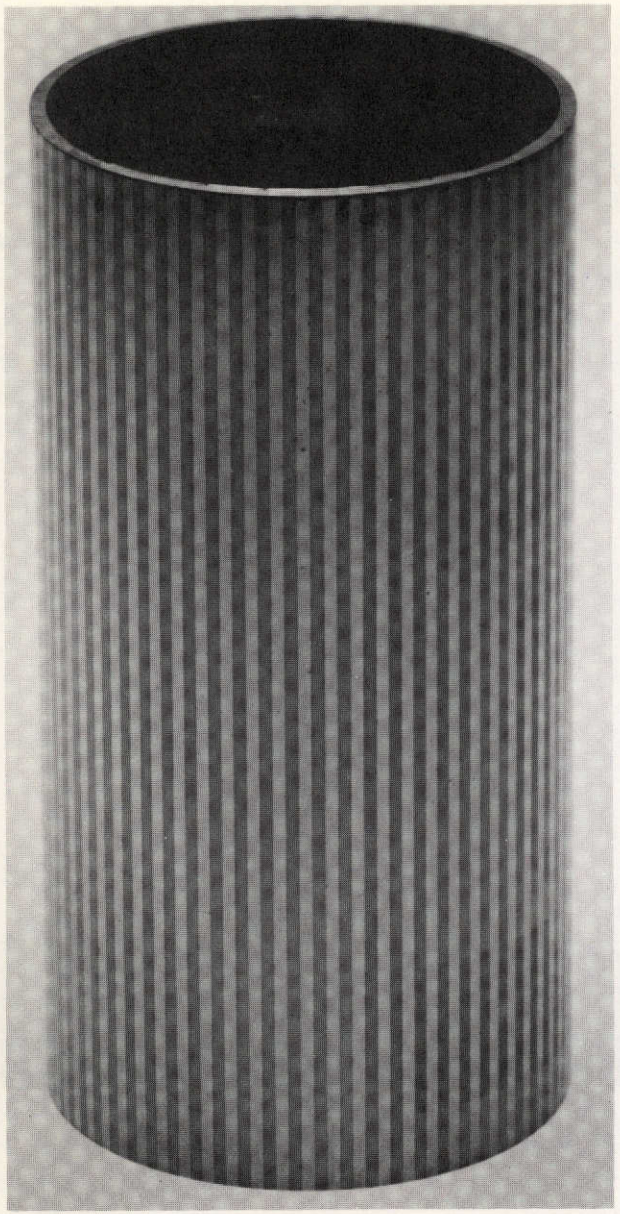

MAG: 1X FE 136193

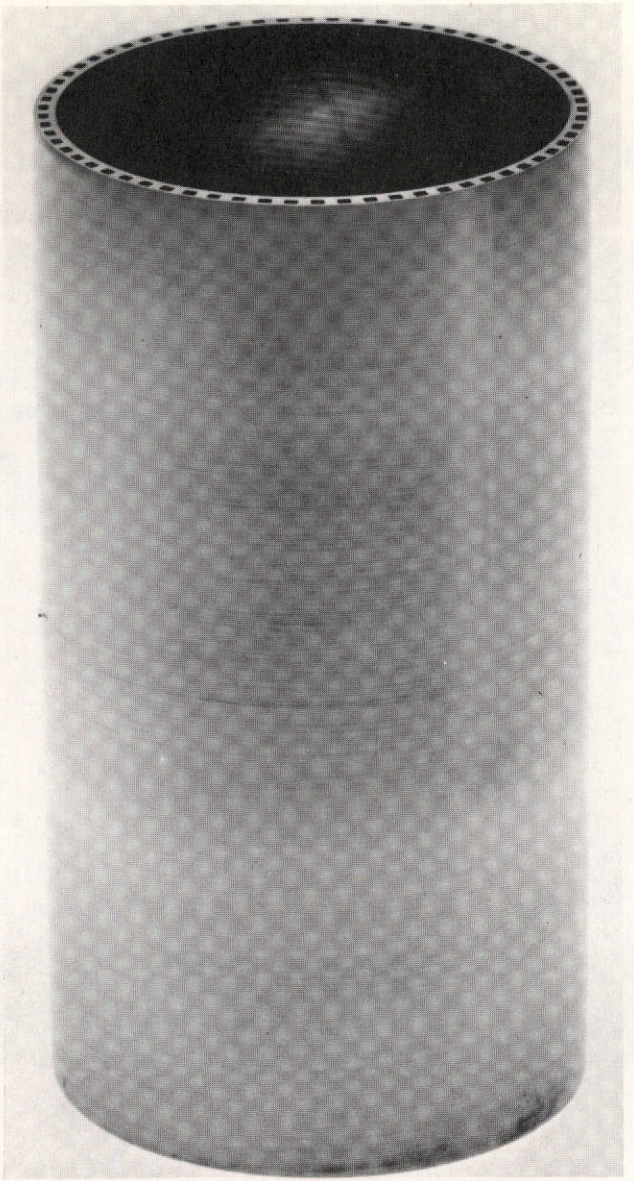

MAG: 1X FE 136194

Figure 31. Appearance of CERROTRU®-Filled Ribbed Wall Cylinder and Final Finished Cylinder FD 78484

The closeout layer was dry lathe machined and finish sanded to a 0.051 ±0.013 cm thickness over the cylinder length. After machining, the CERROTRU filler was removed by the techniques described earlier. Approximately 300s were required to remove to melt out the filler material. The appearance of the as-machined filler cylinder and the final finished cylinder is shown in figure 31. Three small surface defects were present on the cylinder after finishing. These were attributed to arc discharges in the sputtering chamber during deposition. Since the finished cylinder was sent to NASA-LeRC for evaluation, a destructive metallographic analysis was not performed.

CONCLUSIONS

Five materials were evaluated in this program with respect to their use as fillers in the sputter fabrication of regeneratively cooled thrust chambers. From this evaluation the following conclusions were drawn:

1. The closeout layers on substrates with the flame sprayed aluminum filler exhibited the highest bond strengths achieved in this program (in excess of 72.3 MN/m^2 (10,500 psi). The porosity resulting from the flame spraying technique was found to be the source of extensive system contamination leading to open closeout layer structures. Fully dense aluminum, although not evaluated in this program, would probably be the most advantageous filler material for the fabrication of thrust chambers.

2. An upward casting technique, developed for filling the grooved cylinders with the low melting alloys, resulted in complete filling of the grooves with CERROBEND and CERROTRU fillers. The high shrinkage of CERROCAST prevented complete filling by the technique employed and hence was eliminated from consideration.

3. CERROBEND was found to be incompatible with the high vacuum environment and excessive bond contamination invariably resulted when this material was used.

4. Of the filler materials evaluated, CERROTRU was the most suitable with respect to filling the grooves and vacuum system compatibility. However, the bond strength of the closeout layer was found to be sensitive to the length and severity of the sputter cleaning operation.

   Complete removal of CERROTRU required etching of the last remnants in a concentrated HCl solution. The observed embrittlement of the sputtered closeout layer after the etching operation was attributed to the open, fibrous nature of the sputtered closeout layers.

5. The slurry-applied SERMETAL 481 was found to be incompatible with the high vacuum environment. Outgassing from the extensive porosity of this material prevented the normal vacuum levels from being obtained.

6. The machining technique used on the filled substrates was shown to influence the occurrence and severity of closeout layer cracks. Of the machining techniques investigated, dry bidirectional lathe machining contributed least to rib edge deformation and opening of the rib wall-filler interface and, therefore, resulted in reducing the occurrence of closeout layer cracking.

7. The final surface preparation technique was shown to influence the formation of defects in the closeout layer. Sanding with 600-grit SiC paper provided the cleanest interfaces and the fewest closeout layer defects. The use of glass peening or heavy vapor blasting introduced surface asperities that contributed to the formation of defects in the closeout layer.

8. The effects of variations in substrate bias on the elimination of structural defects in the sputtered closeout layer could not be ascertained due to concurrent variations in the filler material, machining, finishing, and cleaning techniques. However, Krypton entrapment was found to be the greatest in those closeout layers applied with the highest substrate bias levels.

9. The substrate temperature during deposition must be kept below approximately 400°K (127°C) if the properties of the OFHC copper substrate are to be retained after long term deposition cycles. At low substrate temperatures, typically less than 366°K (93°C), low rate depositions must be performed to eliminate open columnar or fibrous grain structures.

REFERENCES

1. McClanahan, E. D., R. Busch, and R. W. Moss, "Property Investigation and Sputter Deposition of Dispersion-Hardened Copper for Fatigue Specimen Fabrication," Final Report, Contract NAS3-17491, 12 November 1973.

2. McCandless, L. C., and L. G. Davies, "Development of Improved Electroforming Technique," NASA CR-134480, November 1973.

3. American Metal Climax, Inc., New York, New York.

4. AIRCO, Inc., Riverton, New Jersey.

5. Cerro Copper and Brass Company, Bellefonte, Pennsylvania.

6. Hysol Division, Dexter Corporation, Olean, New York.

7. Teleflex, Inc., Sermetel Division, North Wales, Pennsylvania.

8. Gill, W. D., and E. Kay, "Efficient Low Pressure Sputtering in a Large Inverted Magnetron Suitable for Film Synthesis," Review of Scientific Instruments, Vol. 36, March 1965, pp. 277-282.

9. Thorton, J. A., "Influence of Apparatus Geometry and Deposition Conditions on the Structure and Topography of Thick Sputtered Coatings," presented at the American Vacuum Society Conference on Structure - Property Relationships in Thick Film and Bulk Coating, 28-30 January 1974, San Francisco, California.